AD

USAAVLABS TECHNICAL REPORT 64-68F

HEAVY-LIFT TIP TURBOJET ROTOR SYSTEM
VOLUME VI
DYNAMIC AND AEROELASTIC STUDIES

October 1965

U. S. ARMY AVIATION MATERIEL LABORATORIES
FORT EUSTIS, VIRGINIA

CONTRACT DA 44-177-AMC-25(T)
HILLER AIRCRAFT COMPANY, INC.

DDC Availability Notices

Qualified requesters may obtain copies of this report from DDC.

This report has been furnished to the Department of Commerce for sale to the public.

Disclaimers

The findings in this report are not to be construed as an official Department of the Army position, unless so designated by other authorized documents.

When Government drawings, specifications, or other data are used for any purpose other than in connection with a definitely related Government procurement operation, the United States Government thereby incurs no responsibility nor any obligation whatsoever; and the fact that the Government may have formulated, furnished, or in any way supplied the said drawings, specifications, or other data is not to be regarded by implication or otherwise as in any manner licensing the holder or any other person or corporation, or conveying any rights or permission, to manufacture, use, or sell any patented invention that may in any way be related thereto.

Disposition Instructions

Destroy this report when it is no longer needed. Do not return it to the originator.

DISCLAIMER NOTICE

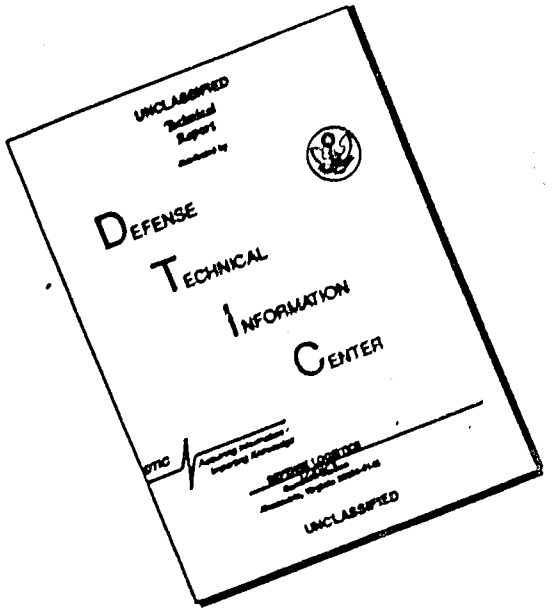

THIS DOCUMENT IS BEST QUALITY AVAILABLE. THE COPY FURNISHED TO DTIC CONTAINED A SIGNIFICANT NUMBER OF PAGES WHICH DO NOT REPRODUCE LEGIBLY.

Task 1M121401D14412
Contract DA 44-177-AMC-25(T)
USAAVLABS Technical Report 64-68F
October 1965

HEAVY-LIFT TIP TURBOJET ROTOR SYSTEM

VOLUME VI

DYNAMIC AND AEROELASTIC STUDIES

Hiller Engineering Report No. 64-46

Prepared by

Hiller Aircraft Company, Inc.
Subsidiary of Fairchild Hiller Corporation
Palo Alto, California

For

U. S. ARMY AVIATION MATERIEL LABORATORIES
FORT EUSTIS, VIRGINIA

(U. S. Army Transportation Research Command when report prepared)

CONTENTS

ILLUSTRATIONS

SYMBOLS

a	Airfoil lift curve slope, /rad.
a_o	Rotor blade precone angle
b	Number of rotor blades
B	Tip loss factor
c	Blade chord
EI	Blade bending stiffness, lb-in^2
g	Gravitational units, 32.2 ft/sec^2
G	Damping factor
GJ	Blade torsional stiffness, lb-in^2
h	Tip engine thrust offset from the blade chord line, in.
I_E	Mass moment of inertia of the engine rotating parts, lb-in-sec^2
ΔI_p	Unit mass moment of inertia of a blade section about a vertical axis through the section feathering axis, lb-in-sec^2/in.
k	Ratio of blade torsional stiffness to root control spring stiffness, $(GJ/R)/k_c$
k_c	Root control spring stiffness, lb-in/rad.
n	Load factor, multiples of g
Q	Torque
r	Radial distance from the rotor centerline of rotation to a point on the blade
R	Rotor radius
T	Rotor thrust, lb.
T_E	Tip engine thrust, lb.
V_T	Tip speed, f.p.s.
W	Weight, lb.

SYMBOLS (CONTINUED)

δ_3	Pitch-flap coupling angle
θ	Blade geometric pitch
θ_T	Blade twist, positive if the geometric angle at the tip is greater than at the root
λ	Rotor inflow parameter
ρ	Air mass density, slugs/ft^3
ψ	Rotor blade azimuth angle, measured in direction of rotation from an aft position in the rotor disk
ω_E, Ω_2	Angular velocity of the engine rotating parts, rad/sec.
Ω, Ω_1	Rotor angular velocity, rad/sec.

1.0 SUMMARY

The studies discussed in this report pertain to dynamic and aeroelastic phenomena of the rotor system for a heavy-lift helicopter employing turbojet engines mounted at the tips of the rotor blades. A majority of the rotor blade frequency and blade flutter boundary work has been accomplished using a lumped mass rotor blade simulation on a direct analog computer and is completely documented in Reference 1. The important results of these studies as well as other dynamic investigations which are necessary to insure adequate helicopter performance are included in this report. The scope of the material covered herein is summarized in the following paragraphs.

1.1 Uncoupled and Coupled Rotor Blade Frequencies

Two independent methods have been used to obtain coupled and uncoupled rotor blade frequencies. The first three uncoupled flapwise, chordwise, and torsional natural frequencies have been calculated using a lumped mass simulation of the rotor blade and employing standard digital computer matrix iteration techniques to obtain both the frequencies and normalized mode shapes. Completely coupled rotor blade frequencies have been experimentally determined using the direct analog computer simulation described in Reference 1. The uncoupled flapwise and chordwise frequencies are plotted versus rotor angular velocity in order to provide a visual picture of frequency placement to avoid rotor speed harmonics. A comparison is also made of the uncoupled and coupled frequencies to determine both the effect of complete coupling on frequencies and to compare the frequencies arrived at by using the two methods mentioned.

1.2 Periodic Engine Thrust

The effect of a periodically changing engine inlet environment for all flight conditions except hover is discussed in terms of engine alternating thrust. It is difficult to treat this problem accurately since the tip engines are to be governed, but a qualitative discussion is presented which points out an order of magnitude of in-plane excitation which could result during forward flight.

1.3 Vibrations Resulting from One Engine Inoperative

The symmetry which exists for the four rotor blades when all eight tip engines are operating properly is obviously destroyed if any one engine fails and the remaining seven continue to operate. Discussions are presented which consider the effect of unsymmetrical in-plane blade deflection as well as unsymmetrical torsional deflection of the blade supporting the inoperative engine as it compares with the other three blades. A hover condition at design gross weight is used for this analysis so that the periodic loads which result with one engine out are not

confused with other periodic loads which result at forward speed. Since this study is directed toward determination of the order of magnitude of excitation which could occur in the case of an engine failure, the hover condition is adequate.

1.4 Mechanical Instability

A discussion pertaining to the avoidance of the phenomenon known as ground resonance is presented. The rotor design under consideration uses the ground resonance avoidance practice of designing for a first in-plane rotating frequency which is above one cycle per revolution of the rotor. Data are presented which show the effect of collective pitch on the first in-plane frequency for the coupled rotor blade simulation of Reference 1. A simplified analysis of the effect of a blade tip-mounted gyroscope (engine rotating parts) is presented so that the effect of this gyroscope on frequency can be estimated. This gyroscope analysis is presented to compare the relative influence on blade frequency of the engine turbine and compressor as a nonrotating mass as opposed to a rotating mass.

1.5 Torsional Divergence

A simplified approach to rotor blade torsional divergence, which assumes no flapwise or in-plane motion of the blade, is presented. The effects of a tip mass and a root control spring are included as well as a tapered blade torsional stiffness. A sample calculation of the rotor tip speed at which torsional divergence would occur is presented using the same blade properties which are used in the rotor blade flutter study.

1.6 Special Dynamic Considerations

Any helicopter is likely to have design concepts which introduce dynamic phenomena peculiar to that helicopter. Two such phenomena are considered in this report. The very low rotor angular velocity makes it possible for the pilot to excite the first in-plane cyclic mode of the blades, and a discussion is presented which describes the condition with comments on the seriousness of the problem. The concept of a heavy-lift helicopter presents the possibility of carrying cargo as a slung load suspended beneath the helicopter. A discussion of the possible influence of this suspended cargo upon blade dynamics is included.

1.7 Rotor Blade Flutter

Reference 1 presents results of a direct analog computer study which includes a variation of parameters investigation of rotor blade flutter. The significant details of this study have been extracted from Reference 1 and are discussed in this report. The methods employed for the determination of flutter boundaries is described as well as the helicopter

flight conditions considered. The influence of root control spring stiffness, tip weight location, pitch-flap coupling (δ_3), blade elastic axis location, tip engine gyroscopics, blade chord and blade stiffness variations on blade aerodynamic damping are discussed.

2.0 CONCLUSIONS

The dynamic and aeroelastic behavior of the four-bladed universally teetering rotor system proposed for the heavy-lift tip turbojet helicopter is discussed and evaluated in this report. The conclusions concerning the dynamic adequacy of the rotor system are outlined in the following paragraphs for all phases of the dynamic investigations presented in this report.

2.1 Uncoupled and Coupled Rotor Blade Frequencies

A comparison of uncoupled and coupled rotor blade frequencies, calculated using independent methods, indicates that flapwise frequencies can be satisfactorily approximated using an uncoupled model of the rotor blade whereas coupling has a more pronounced effect on in-plane frequencies. The frequency of primary interest from both a loading and dynamic point of view is the first cyclic in-plane frequency. The flapwise/in-plane coupling increases with collective pitch to reduce this frequency by 16 percent from minimum to maximum collective pitch settings.

The natural frequency study presented in Reference 1 shows that the first six coupled cyclic and collective modes avoid resonance with their respective airload excitation harmonics throughout the collective pitch range.

2.2 Periodic Engine Thrust

The thrust of the tip engines will vary periodically with rotor azimuth position for all helicopter flight conditions except hover and vertical flight. The magnitude and phasing of this thrust variation will depend largely upon the engine-governor dynamics, which have not been thoroughly investigated at this time. The quantitative effect of engine inlet velocity changes on the engine alone is to change the engine thrust by a lesser amount than the periodic variation of engine nacelle drag, and so the thrust variation should not be of primary concern.

2.3 Vibrations Resulting from One Engine Inoperative

The loss of one engine in flight would cause an in-plane circular motion of the rotor system and an out-of-track condition. The in-plane motion at one cycle per rotor revolution would result from a rotor system center-of-gravity movement away from the centerline of rotation due to unsymmetrical in-plane bending of the four blades. The rotating load due to this center-of-gravity displacement is in phase with the rotating unbalanced engine thrust vector. The net load for a hover condition at design gross weight will probably not exceed 2,000 pounds, which is small compared with the gross weight of the aircraft. With an adequate rotor isolation system, this rotating force should be virtually unfelt in the fuselage.

The out-of-track condition would result from a pitch angle change on only the one blade supporting the inoperative engine. The helicopter roughness which would result, however, is not expected to be more severe than that caused by occasional out-of-track conditions for smaller helicopters.

2.4 Mechanical Instability

Ground resonance, which is caused by a first cyclic in-plane natural frequency which is close to one cycle per rotor revolution, will be avoided with the proposed helicopter by designing the rotor blades to have a first cyclic in-plane frequency well above one cycle per revolution. Increasing collective pitch tends to lower this frequency due to flapwise/in-plane coupling, and so design steps have been taken to assure a frequency margin throughout the collective pitch range. The influence of the engine rotating parts is shown to have negligible effect upon this frequency.

2.5 Torsional Divergence

The prospective location of the rotor blade shear center ahead of the blade section center of pressure makes the pure torsional divergence problem nonexistent. The torsional stiffnesses of the proposed rotor blade and root control spring, however, are large enough that the divergence tip speed would be far above normal rotor speed even if the shear center were located 15 percent of the chord aft of the center of pressure.

2.6 Special Dynamic Considerations

Due to the low first cyclic in-plane natural frequency of the rotor blades, it is well within pilot capability to perform a cyclic stick whirl which will excite this mode. This condition cannot be avoided and so is considered a design condition.

The possibility of carrying cargo which is slung beneath the helicopter has been investigated from the standpoint of dynamic coupling with rotor blade frequencies. The frequency of oscillation of such a sling load would be so far below any frequencies of the rotor system that no effects on rotor dynamics are expected.

2.7 Rotor Blade Flutter

The rotor system as presently designed possesses positive damping for all modes of vibration investigated in Reference 1. A variation of parameters study on blade flutter points out the following damping changes as functions of parameter changes.

a) The second cyclic mode (first in-plane mode) would be the first mode

to become unstable with decreasing root control spring stiffness. This spring would have to be about 0.1 of its design stiffness to approach the stability boundary.

b) A chordwise movement of the blade tip mass from the nominal design location (0.22 chord) affects the damping of various modes in different ways. In no case does the blade flutter for center-of-gravity locations between 16 percent and 28 percent of the chord.

c) An increase in pitch-flap coupling (δ_3 angle) decreases the aerodynamic damping of the second cyclic mode. For a structural damping factor of .03, however, this mode should be stable for δ_3 angles up to 45 degrees.

d) The aerodynamic damping is relatively unchanged with small chordwise variations in blade shear center.

e) The rotational speed and direction of rotation of the engine rotating parts have a negligible effect upon flutter boundaries.

f) Increased blade chord provides an increase in aerodynamic damping for a majority of the modes of vibration but has a slight destabilizing effect on the second cyclic, sixth cyclic, and the sixth collective modes.

g) A flapwise blade stiffness increase at the root of the blade has negligible effect on damping.

3.0 RECOMMENDATIONS

The following recommendations are presented to complement the analytical studies already conducted and discussed in this report.

a) It would be advantageous to study the dynamic consequences of engine failure operation using actual hardware. The necessity of pilot corrective action (such as shutting down an engine on the opposing blade) can best be determined on a flight vehicle or whirl stand.

b) A cyclic control whirl study using actual hardware should be performed to determine the in-plane bending moments which result from this maneuver. Since these moments are inversely proportional to structural damping, it is necessary to determine whether Reference 1 is unconservative by assuming that G = .03.

c) The flutter analyses performed in Reference 1 were all conducted for normal gross weight. Since the ratio of minimum flying weight to normal gross weight is relatively low for this helicopter, additional low inflow flutter studies should be performed to insure flutter stability when operating at lower gross weights.

4.0 DYNAMIC, AEROELASTIC, AND FLUTTER STUDIES

In order to make possible a complete parametric study of rotor blade dynamics, a direct analog computer simulation was made of the tip turbojet rotor system, and results from these studies are recorded in Reference 1. Due to the availability of this analog simulation, several dynamic studies, not directly related to blade flutter, were performed to complement the calculated data pertaining to uncoupled blade motion.

4.1 Rotor Blade Frequencies

The flapwise, in-plane, and torsional natural frequencies of the rotor blades have been determined both for uncoupled motion with the blade in flat pitch and for completely coupled motion, including aerodynamic effects, on the direct analog computer. Preliminary work in this area was concentrated on achieving a sufficiently high first in-plane frequency so as to avoid ground resonance problems as well as large chordwise loads due to one-cycle-per-revolution harmonic loads. The remaining frequencies were determined in ensuing work, and blade properties were adjusted accordingly to avoid resonance with rotor speed harmonics larger than one cycle per revolution.

4.1.1 Uncoupled Frequencies

The first three uncoupled flapwise, chordwise, and torsional frequencies have been calculated using the blade properties plotted in Figures 5 and 6. The flapwise and chordwise frequencies were calculated using a ten-station lumped-mass simulation of the rotor blade and standard matrix iteration procedures such as those in Reference 2. The matrix iteration procedure produces a normalized mode shape for each frequency and the effects of centrifugal force are included. Figures 9 and 10 show the first three rotating flapwise and chordwise uncoupled natural frequencies as functions of rotor speed. The torsional uncoupled natural frequencies of the rotor blade have been calculated using the equivalent torsional system shown in Figure 11 wherein the blade and tip mass pitching inertias are lumped into seven concentrated masses connected by weightless torsional springs which represent the rotor blade torsional stiffness. A root spring of $100(10)^6$ inch-pounds per radian is used to simulate the nominal control system stiffness as required by the current design.

The three flapwise frequencies plotted in Figure 9 are, in order of increasing magnitude, the first collective (or built-in) mode, the first cyclic mode, and the second collective (or built-in) mode. The definitions of built-in, cyclic, and collective modes are found in Reference 1 and pertain to root restraint conditions. A comparison of the frequencies in Figure 9 at nominal hovering tip speed with the results in Reference 1 for the blade tip angle of 0 degrees shows the following.

Mode	Figure 9	Reference 1	Critical Excitation Harmonics	Nearest Excitation Harmonic
	(Cycles/Revolution)			
Collective	1.20	1.18	2,4,6,8,10,....	2
Cyclic	3.50	3.30	1,3,5,7, 9,....	3
Collective	4.70	4.40	2,4,6,8,10,....	4

The three chordwise frequencies plotted in Figure 10 are, in order of increasing magnitude, a cyclic (or built-in) mode, a collective mode, and a cyclic (or built-in) mode. A comparison of the frequencies in Figure 10 at nominal hovering tip speed with the results in Reference 1 for the blade tip angle of 0 degrees shows the following.

Mode	Figure 10	Reference 1	Critical Excitation Harmonics	Nearest Excitation Harmonic
	(Cycles/Revolution)			
Cyclic	1.38	1.36	1,2,3,5,6,7,....	1
Collective	6.81	5.94	0,4,8,12, ...	4 or 8
Cyclic	10.10	9.12	1,2,3,5,6,7,....	9

A comparison of the uncoupled frequencies of Figures 9 and 10 with the completely coupled frequencies in Reference 1 shows adequate agreement (less than 7-percent difference) for flapwise modes, while the chordwise modes show that coupling has a more pronounced effect on in-plane frequencies.

The first three nonrotating, uncoupled torsional frequencies of the rotor blade have been calculated using the equivalent torsional system shown in Figure 11. Comparison of the first natural frequency with that of Reference 1 shows that centrifugal force has only a small effect on torsional frequency and, hence, no effort has been made to calculate these torsional natural frequencies at nominal hovering tip speed. The first three torsional natural frequencies are as follows:

Mode	Uncoupled (Nonrotating)	Reference 1 (Rotating)	
First	7.54	8.24	Cycles/Revolution
Second	22.0	--	" "
Third	39.5	--	" "

The nonrotating frequencies are given as cycles per revolution at nominal hovering tip speed for comparison with Reference 1 data.

4.1.2 Coupled Frequencies

All rotor blade coupled natural frequency work has been accomplished on a direct analog computer using the blade properties plotted in Figures 5 and 6, with the results being tabulated and plotted in Reference 1. The scope of the studies discussed in Reference 1 is far too large to repeat in this report, but the first six natural frequencies for each of the blade root restraint conditions are repeated in Table 1 for convenience. The selected conditions represent zero forward flight conditions which include aerodynamics, centrifugal force effects (for nominal hovering tip speed), and engine gyroscopic effects. These conditions are summarized in Table 4, but it must be kept in mind that the condition entitled "Maximum Negative Collective Pitch" is a fictitious condition used only for the flutter study since the lower limit for collective pitch is envisioned to be 0 degrees at 0.75 radius and not -5 degrees.

TABLE 1
COUPLED NATURAL FREQUENCIES

Mode \ Condition		1g Hover	2.5g Hover	Maximum Vertical Climb	Maximum Negative Collective Pitch
Cyclic	z-1	1.09	1.09	1.10	1.09
↓	x-1	1.24	1.12	1.18	1.18
	z-2	3.52	3.68	3.61	3.40
	z-3	7.30	7.02	7.17	7.38
	θ-1	8.35	8.58	8.57	8.25
	x-2	8.86	8.84	8.84	9.05
Collective	z-1	1.25	1.26	1.25	1.24
↓	z-2	4.53	4.48	4.51	4.51
	x-1	5.87	5.87	5.90	5.90
	θ-1	8.22	8.14	8.18	8.11
	z-3	9.57	9.52	9.49	9.56
	z-4	14.68	14.49	14.39	15.46
Built-In	z-1	1.18	1.11	1.14	1.25
↓	x-1	1.38	1.48	1.40	1.36
	z-2	4.53	4.50	4.53	4.53
	θ-1	8.24	8.08	8.24	8.11
	x-2	8.90	8.86	8.90	8.87
	z-3	9.67	9.62	9.58	9.73

All frequencies are given in cycles per revolution at nominal hovering rotor speed. The mode designations are defined in Reference 1 and, in general, specify flapwise modes (z), in-plane modes (x), and torsional modes (θ).

Reference 1 also presents data which shows the effect of collective pitch on coupled flapwise and in-plane frequencies which are located nearest to critical excitation harmonics. This investigation was conducted with no aerodynamics on the rotor blade and tip engines inoperative so as to show the coupling effect of variable collective pitch only. Figure 12 is a composite copy of the curves in Reference 1 which summarize this study. These curves show that both the first cyclic in-plane mode and the third cyclic flapwise mode are nearer to their critical excitation harmonics for large values of collective pitch than they are for flat pitch or lg hovering collective pitch, but neither curve crosses its resonance harmonic. Reference 1 also points out that this collective pitch coupling which degrades the first cyclic in-plane mode can be minimized by increasing the flapwise stiffness in the root area. This fact has influenced the root stiffness buildup shown in Figure 5.

4.2 Periodic Engine Thrust

Each of the four blades experiences a one cycle per rotor revolution induced and profile drag excitation when the helicopter is in forward flight due to the variation of tip speed and induced velocity with azimuth. Since the engines operate on the tips of the rotor blades, they can be expected to experience a periodic thrust variation due to variable engine inlet velocity occurring in forward flight.

The turbojet engines are to be governed to maintain constant rotor speed and the governing device, in combination with the ungoverned engine dynamics, will influence this periodic engine thrust. No literature or completed studies are available at this time to evaluate this phenomenon, but an order of magnitude calculation can be made to establish the significance of this excitation source.

If the rotor tip speed is assumed to be 592 feet per second in forward flight and the helicopter is flying at its maximum design level flight speed of 125 miles per hour, the relative engine inlet velocities of the advancing blade (ψ = 90 degrees) and the retreating blade (ψ = 270 degrees) are as follows:

$$V_{90} = 592 + \frac{88(125)}{60} = 775 \text{ f.p.s.}$$

$$V_{270} = 592 - \frac{88(125)}{60} = 409 \text{ f.p.s.}$$

If it were further assumed that the engine component transfer functions have sufficiently small time delay characteristics so that engine reaction time to inlet velocity changes is small when compared with the time

required for one rotor revolution (0.59 second), then the engine thrust variation can be estimated from standard engine thrust curves. For a constant turbine speed, the engine thrust change between inlet velocities of 409 feet per second and 775 feet per second would be from approximately 1,520 pounds of thrust to 1,580 pounds for maximum turbine speed. The aerodynamic nacelle drag variations with azimuth in forward flight are larger than the combined thrust variations of both engines on one blade tip and, hence, periodic engine thrust variations appear to be second order quantities.

4.3 Vibrations Resulting from One Engine Inoperative

4.3.1 In-Plane Excitation

There are several possible courses which may be taken in the event of engine failure. One of these might be a pilot-performed action of shutting down the corresponding engine on the opposing blade so as to bring engine thrust forces and blade deflected positions into a state of symmetry and thus avoid force unbalance in the rotating system. Another course of action would be to continue engine governing to maintain rotor speed, in which case the remaining engines would be required to deliver more thrust. This second alternative, of course, would result in unbalanced in-plane forces in the rotating system and would add to the roughness of flight to some degree. The forces resulting from this second alternative are considered here with their possible consequences.

If the helicopter is assumed to be hovering at design gross weight and normal hovering tip speed (650 feet per second), the engine thrust required for equilibrium is 1,010 pounds per engine, or 8,080 pounds total for eight tip engines. If the remaining seven engines following an engine failure are assumed to be governed exactly alike until equilibrium is restored, each of these engines must increase its thrust to 8,080/7 = 1,154 pounds. Including a nacelle drag on each blade tip of 316 pounds, the equilibrium rotor configuration would appear similar to that shown in Figure 1.

A summation of moments about the centerline of rotation in Figure 1 verifies equilibrium for R = 56 feet as follows:

$$M = 672\left[3(1,992) + 858\right] - 4\int_0^{672} 10.14\left(\frac{r}{672}\right)^2 r\,dr$$

$$M = 4,579,008 - 10.14(672)^2$$

$$M = 4,579,008 - 4,579,062 \approx 0$$

Using the chordwise stiffness curve in Figure 5, the in-plane deflection of each blade can be calculated for the loads shown in Figure 1. Then using the blade weight distribution in Figure 6 along with a tip weight of 1,200 pounds on each blade, a center-of-gravity movement away from the centerline of rotation can be estimated. Performing this calculation indicates a center-of-gravity movement of 0.13 inches in the 0-degree azi-

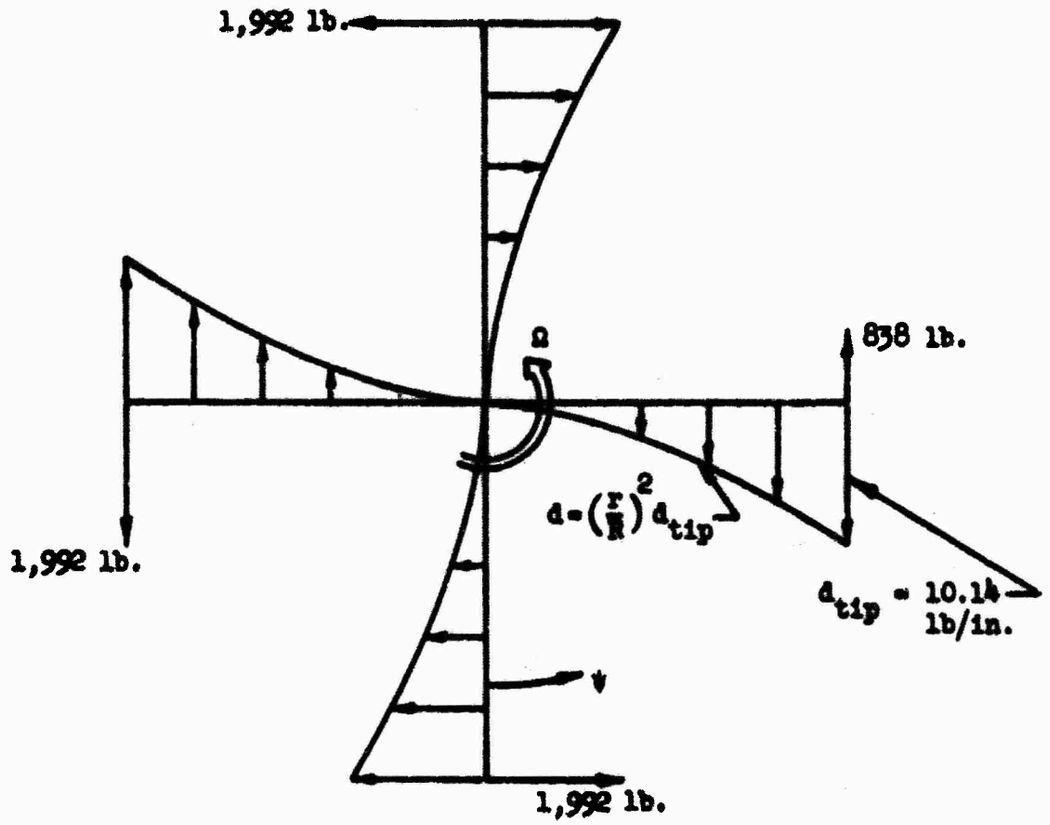

Figure 1. Rotor Equilibrium, One Engine Inoperative.

muth direction if the blade with one engine inoperative is assumed to be in the 90-degree azimuth position shown in Figure 1. Since a summation of engine thrust vectors gives an unbalanced force of 1,154 pounds at the centerline of rotation and in the 0-degree azimuth direction, the rotating centrifugal force vector due to a displaced center of gravity is in phase with the rotating engine thrust vector giving a total rotating load at the rotor hub as follows:

$$F = \frac{W_{RG}}{g} \delta\Omega^2 + \Delta T_E$$

where: W_{RG} = total rotor group weight, lb.
δ = center of gravity displacement, in.
Ω = rotor angular velocity, rad/sec.
ΔT_E = unbalanced engine thrust, lb.

$$F = \frac{W_{RG}(0.13)(650)^2}{386(56)^2} + 1{,}154 = .0454\, W_{RG} + 1{,}154 \text{ lb.}$$

The rotor group weight is less than 20,000 pounds and so the rotating force vector due to one engine out in hover should not exceed 2,000 pounds.

The dynamic consequences of this rotating force vector are not unlike the harmonic loads at the rotor hub created in forward flight. If the isolation between the rotating mass and the suspended mass (fuselage) resulted in a natural frequency close to one cycle per revolution of the main rotor, the effect of the rotating force could be amplified to the extent of creating uncomfortable load factors in the suspended mass. With adequate rotor isolation, however, this rotating force at the rotor hub should be virtually unfelt in the fuselage.

4.3.2 Flapwise Excitation

In addition to the in-plane excitation which could result with one engine inoperative, there is also a possibility of vertical excitation at the rotor hub caused by an out-of-track condition. The rotor blades are designed to incorporate a 10-degree, built-in twist. The failure of one or both of the tip engines on any blade will result in a change in torsion at the blade tip and hence a change in effective twist of the blade. In order to evaluate the effect of an engine failure, it is necessary to calculate the change in blade twist. Consider Figure 2 as representing a segment of a rotor blade which is dr inches in length and located a distance of r inches from the centerline of rotation.

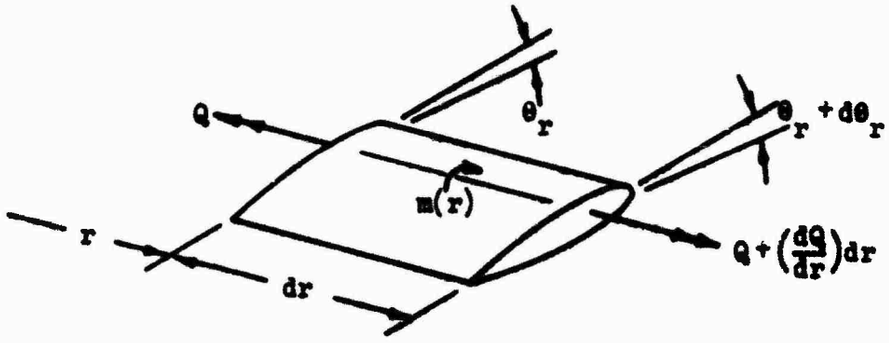

Figure 2. Rotor Blade Section.

By definition:

θ_r = Geometric blade pitch, + nose up, rad.

θ_T = Built-in blade twist, + when tip angle exceeds root angle, rad.

m(r) = Torsion due to section centrifugal centering and rigid blade coning, + nose down, in-lb.

It can be written that $\theta_r = \theta'_r + \frac{r}{R}\theta_T$ (1)

where θ'_r can be thought of as being the geometric blade pitch at station r if the blade had no built-in twist.

Then: $\theta_r + d\theta_r = \theta'_r + \frac{Q}{GJ}dr + \frac{r+dr}{R}\theta_T$ (2)

Subtracting (1) from (2) and dividing by dr gives

$$\frac{d\theta_r}{dr} = \frac{Q}{GJ} + \frac{1}{R}\theta_T \quad (3)$$

Differentiating (1) gives

$$\frac{d\theta_r}{dr} = \frac{d\theta'_r}{dr} + \frac{1}{R}\theta_T \quad (4)$$

Equating (3) and (4) gives

$$\frac{Q}{GJ} = \frac{d\theta'_r}{dr} - \frac{d\theta_r}{dr} - \frac{1}{R}\theta_T$$

from which it follows that

$$\frac{d^2\theta'_r}{dr^2} = \frac{d^2\theta_r}{dr^2} - \frac{(dQ/dr)}{GJ} \quad (5)$$

But: $m(r) = dQ/dr = \Delta I_p \Omega^2 \theta_r + m_o a_o \bar{x} \Omega^2 r$

$$m(r) = dQ/dr = \Delta I_p \Omega^2 \theta'_r + \frac{\Delta I_p \Omega^2 r}{R}\theta_T + m_o a_o \bar{x} \Omega^2 r \quad (6)$$

where:

ΔI_p = mass moment of inertia of the section about a vertical axis through the section center of gravity, in-lb-sec^2.

m_o = mass of the blade section, lb-sec^2/in.

a_o = rotor blade coning angle, rad.

$\bar{x}$ = blade section center of gravity with respect to the feathering axis, + forward, in.

Ω = rotor angular velocity, rad/sec.

Substituting (6) into (5) and rearranging gives:

$$\frac{d^2\theta'_r}{dr^2} - \frac{\Delta I_p \Omega^2}{GJ}\theta'_r = -\frac{\Delta I_p \Omega^2 r}{GJR}\theta_T + \frac{m_o a_o \bar{x} \Omega^2}{GJ} r \quad (7)$$

Denoting $\eta^2 = \frac{\Delta I_p \Omega^2}{GJ}$ and $\lambda = \frac{m_o a_o \bar{x} \Omega^2}{GJ}$

Equation (7) can be written as

$$\frac{d^2\theta'_r}{dr^2} - \eta^2\theta'_r = \left(\frac{\eta^2\theta_T}{R} + \lambda\right)r \tag{8}$$

Equation (8) has the known solution

$$\theta'_r = A \cosh \eta r + B \sinh \eta r - \left(\frac{\theta_T}{R} + \frac{\lambda}{\eta^2}\right) r \tag{9}$$

The boundary conditions for the blade are:

$$\text{At } r = 0 \text{ (root)}, \quad Q_o = -k_c(\theta_c - \theta_o)$$

$$\text{At } r = R \text{ (tip)}, \quad Q_R = GJ\left(\frac{d\theta'_r}{dr}\right)_R$$

where: θ_c = collective pitch input by pilot, rad.

k_c = control spring at collective pitch input horn, in-lb/rad.

Now, imposing the boundary condition gives:

$$A - \frac{GJ\eta}{k_c} B = \theta_c - \frac{GJ}{Rk_c}\theta_T - \frac{GJ}{\eta^2 k_c}\lambda \tag{10}$$

$$A + \operatorname{ctnh} \eta R = \left(\frac{\theta_T}{\eta R} + \frac{\lambda}{\eta^3} + \frac{Q_R}{\eta GJ}\right) \operatorname{csch} \eta R \tag{11}$$

Denoting $k = \frac{GJ/R}{k_c}$

and solving (10) and (11) for A and B leads to the following general equation for geometric blade pitch at the tip of the rotor blade, or:

$$\theta_R = \theta_T + \frac{\theta_c - k\theta_T - \frac{kR\lambda}{\eta^2} + \left[\left(\theta_T + \frac{\lambda R}{\eta^2}\right)\left(\frac{1}{\eta R} - kR\eta\right) + \frac{Q_R}{\eta GJ}\right]\sinh \eta R + \left[\left(\theta_T + \frac{\lambda R}{\eta^2}\right)(k-1) + \frac{Q_R}{k_c}\right]\cosh \eta R}{\cosh \eta R(1 + k\eta R \tanh \eta R)} \tag{12}$$

The concentrated torque at the blade tip, Q_R, is composed of gyroscopic moments, one-engine-out operation moment, rigid coning moment due to the tip mass, and centrifugal centering moment due to the tip mass.

Before quantitatively considering the torque at the rotor tip, Q_R, Equation (12) can be used to obtain the effect of one- or two-engine-out operation on the geometric pitch at the blade tip as follows:

$$\frac{\partial \theta_R}{\partial Q_R} = \frac{\frac{\sinh \eta R}{\eta GJ} + \frac{\cosh \eta R}{k_c}}{\cosh \eta R(1 + k\eta R \tanh \eta R)} \quad \frac{\text{rad.}}{\text{in-lb.}} \tag{13}$$

The blade parameters of interest are:

$GJ = 6.5(10^9)$ lb-in^2 (effective)
$R = 672$ in.
$\Delta I_p = 2.4$ lb-in-sec^2 (per in.)
$\Omega = 11.6$ rad/sec. (nominal hovering rotor speed)
$\bar{x} = 0$ (balanced blade)
$m_o e_o$ = superfluous since $\bar{x} = 0$

Therefore:

$$\eta = \Omega\sqrt{\frac{\Delta I_p}{GJ}} = 0.000225 \text{ per in.}$$

$\lambda = 0$
$\eta R = 0.150$

$\sinh \eta R = 0.1506$
$\cosh \eta R = 1.0113$
$\tanh \eta R = 0.1489$

and $$k = \frac{GJ/R}{k_c} = \frac{9,675,000}{k_c}$$

$$\frac{\partial \theta_R}{\partial Q_R} = \frac{\frac{1}{9,625,000} + \frac{1.0113}{k_c}}{1.0113 + \frac{218,500}{k_c}} \quad \frac{\text{rad.}}{\text{in-lb.}}$$

Or, expressing θ_R in degrees,

$$\frac{\partial \theta_R}{\partial Q_R} = \frac{\frac{1}{168,000} + \frac{57.94}{k_c}}{1.0113 + \frac{218,500}{k_c}} \quad \frac{\text{deg.}}{\text{in-lb.}} \tag{14}$$

The rigid coning and centrifugal centering torques at the blade tip are functions of the tip mass location with respect to blade feathering axis and the mass moments of inertia and, hence, will not change with engine turbine speed. The gyroscopic torque and torque due to vertically displaced engine thrust with one engine inoperative are, therefore, the only

concentrated torque changes involved for engine failure conditions. The torque change caused by the three possible types of engine failure are as follows:

Two Engines Inoperative:

$$\Delta Q_R = +2 I_E \omega_E \Omega = +2(1.67)(2120)(11.6) = +82{,}100 \text{ in-lb.}$$

Lower Engine Inoperative:

$$\Delta Q_R = +I_E \omega_E \Omega - hT_E = +1.67(2120)11.6 - 13.5(1010)$$

$$\Delta Q_R = +27{,}400 \text{ in-lb.}$$

Upper Engine Inoperative:

$$\Delta Q_R = +I_E \omega_E \Omega + hT_E = +1.67(2120)11.6 + 13.5(1010)$$

$$\Delta Q_R = +54{,}700 \text{ in-lb.}$$

where: I_E = mass moment of inertia of engine rotating parts, = 1.67 in-lb-sec^2 per engine.

ω_E = rotational speed of engine rotating parts, = 20,250 r.p.m. (reference Table 4).

Ω = nominal hovering rotor speed = 11.6 rad/sec.

h = vertical displacement of tip engines from the blade chord line, = ±13.5 in.

T_E = engine thrust required to maintain nominal hovering tip speed, = 1010 lb. per engine (reference Table 4).

Solving for blade tip geometric pitch change, $\Delta\theta_R$, versus root control spring stiffness, k_c, results in the data presented in Table 2 and plotted in Figure 13.

TABLE 2
ENGINE FAILURE EFFECTS ON BLADE TWIST

Control Stiffness, k_c (in-lb/rad.)	Blade Tip Pitch Change, $\Delta\theta_R$ (Degrees)		
	Both Engines Inoperative	Lower Engine Inoperative	Upper Engine Inoperative
∞	+0.483	+0.161	+0.322
10^9	.488	.163	.325
10^8	.529	.177	.353
10^7	.933	.312	.622
10^6	4.265	1.424	2.842

It is obvious from Figure 13 that a control spring stiffness, k_c, in excess of 10^8 inch-pounds per radian results in a negligible difference in pitch change at the blade tip from that which would occur if the control spring is infinitely stiff. The studies in Reference 1 were conducted using $k_c = 10^8$ inch-pounds per radian which resulted in desirable dynamic characteristics of the rotor blades. This value of control spring stiffness for the blade pitch mechanism is chosen as the design goal.

In order to evaluate vertical roughness of the helicopter caused by an engine failure, it is conservative to assume that both engines on one blade become inoperative and that all other engines are kept operative so as to maintain a condition of dissymmetry.

It will be assumed that most of the torsional deflection of the blade changes the apparent twist of the blade and that the root geometric pitch does not change. This is very closely the case with such a stiff root spring. The rotor thrust developed by a hovering helicopter can be simply written as follows:

$$T = \frac{1}{2}\rho abcR\,V_T^2\left[\left(\frac{B^2}{2}\right)\lambda + \left(\frac{B^3}{3}\right)\theta_o + \left(\frac{B^4}{4}\right)\theta_T\right] \qquad (15)$$

where:

ρ = sea level air density, .002378 slugs/ft^3
a = blade section lift curve slope, 5.73/rad.
b = number of blades
c = blade chord, 6.5 ft.
R = rotor radius, 56 ft.
V_T = hovering tip speed, 650 f.p.s.
B = tip loss factor; use B = 1 for simplicity
λ = induced inflow angle, rad.
θ_o = collective pitch at blade root, rad.
θ_T = blade twist, -10 deg.

Solving for the thrust of one blade (b = 1) and noting that by definition

$$\lambda = -\frac{1}{BV_T}\sqrt{\frac{T}{2\rho\pi R^2}}$$

it can be shown that

$$T_{b=1} = \frac{\rho acV_T^2}{192\pi}\left[32\pi R\theta_o + 24\pi R\theta_T + 3ac - \sqrt{9a^2c^2 + 192ac\pi R\theta_o + 144ac\pi R\theta_T}\right]$$

Differentiating to find the thrust change (per blade) per unit change in blade twist, θ_T, gives:

$$\frac{\partial T_{b=1}}{\partial \theta_T} = \frac{\rho a c R V_T^2}{6}\left[1 - \frac{3ac}{\sqrt{9a^2c^2 + 192ac\times\theta_0 + 144ac\times\theta_T}}\right] \quad \frac{\text{lb.}}{\text{rad.}} \qquad (16)$$

Using θ_0 = 16 degrees (Reference Table 4) and substituting the parameters defined for Equation (15) gives:

$$\frac{\partial T_{b=1}}{\partial \theta_T} = 261{,}940\left[1 - \frac{111.74}{\sqrt{199{,}160}}\right] = +196{,}350 \text{ lb/rad.}$$

Since from Table 2 the effective change of blade twist due to both engines inoperative on one blade tip should not exceed +0.529 degrees, the change of lift on the blade which supports the inoperative engines is:

$$\Delta T_{b=1} = +196{,}350\left(\frac{0.529}{57.3}\right) = +1810 \text{ lb.}$$

This value of lift change is conservative due to the simplifying assumption that tip loss factor, B, equals 1.0 instead of a more conventional value such as 0.97.

The consequence of this lift change on one of the four blades can qualitatively be seen to cause an out of track condition since the tip path of this "unpowered" blade will be above the tip paths of the three "powered" blades when viewed at any constant azimuth position. The dynamic effect of this condition on helicopter roughness is considered to be no more severe than out-of-track conditions encountered on other smaller helicopters.

4.4 Mechanical Instability

Aside from the obvious advantages of designing rotor blades so that their natural frequencies do not coincide with airload harmonics which would amplify rotor blade stress levels, it is also advantageous to design the rotor blades so that their first in-plane rotating natural frequency is above one cycle per revolution of the main rotor. This design criterion will permit avoidance of the mechanical instability known as ground resonance without the use of blade dampers which can add undue empty weight to a helicopter.

Efforts were made in preliminary design studies to achieve a first in-plane rotating natural frequency of 1.30 at nominal hovering rotor speed. The flapwise-chordwise coupling phenomenon evaluated in Reference 1, at large collective pitch angles, indicated that it would be wise to increase the uncoupled in-plane frequency so that there would still be adequate frequency margin at high collective pitch settings to avoid ground resonance. The in-plane rotating natural frequencies tabulated in Reference 1 range from 1.36 cycles per revolution in flat pitch to approximately 1.15 cycles per revolution for the blade at its maximum collective pitch setting of 15 degrees at 0.75R.

The use of tip-mounted turbojet engines raises the question as to whether or not the gyroscopic moments at the blade tip affect this in-plane frequency so as to enhance the possibility of ground resonance. Reference 1 presents tabulated frequencies for several flight conditions, each of which is analyzed with tip engines operating and not operating. These studies showed that the tip engine gyroscopics do not affect the first in-plane rotating natural frequency. In addition to the direct analog computer study, an analysis of the gyroscopic contribution of the engines to rotor blade dynamics has been conducted on a simplified model of the rotor blade. The method used is based on a linearized, small damping approximation to simplify the analysis.

The equations of motion of a linear dynamic system may be written in matrix form as follows:

$$[m]\{\ddot{q}\} + [D]\{\dot{q}\} + [k]\{q\} = \{Q\} \tag{17}$$

where:

- $[m]$ is the mass matrix
- $[D]$ is the damping matrix
- $[k]$ is the stiffness matrix
- $\{q\}$ is the generalized coordinate vector
- $\{Q\}$ is the generalized force vector

The gyroscopic damping matrix (commonly called the gyroscopic coupling matrix) can be found by considering the simplified model of Figure 3.

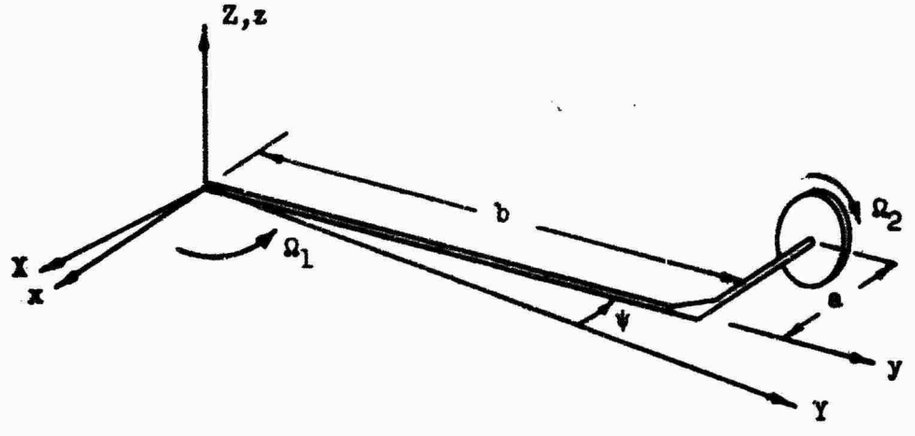

Figure 3. Cantilever Bent.

The rotating parts of both engines are lumped into one gyroscopic disk, which is placed on the end of a weightless, elastic cantilever bent, as shown.

For purposes of this analysis, consider the following definitions:

m = mass of the gyroscopic disk.

I_1 = mass moment of inertia of the disk about an axis in the plane of the disk (i.e., one of the disk diametral axes).

I_2 = mass moment of inertia of the disk about an axis perpendicular to the plane of the disk (i.e., the polar mass moment of inertia).

x,y,z = the moving axes defined in Figure 3.

X,Y,Z = fixed axes in space.

EI_x = uniform bending stiffness of the cantilever bent in the plane of rotor rotation (i.e., the chordwise stiffness of the blade).

EI_z = uniform bending stiffness of the cantilever bent out of the plane of rotor rotation (i.e., the flapwise stiffness of the blade).

GJ = uniform torsional stiffness of the cantilever bent.

a,b = dimensions which position the gyroscopic disk with respect to the cantilever bent and the rotor centerline of rotation (see Figure 3).

θ = the angular rotation of the plane of the disk about the y axis (i.e., pitching angle), + nose up.

ϕ = the angular rotation of the axis of the disk about the x axis (i.e., flapping angle), + upward.

ξ = the angular rotation of the plane of the disk about the z axis (i.e., lead-lag angle), + forward.

Ω_1 = rotor angular velocity.

Ω_2 = disk angular velocity about its own axis of rotation.

Writing the equations of equilibrium of the system shown in Figure 3 produces the following linearized equations.

Σ forces parallel to the x axis at center of the disk:

$$+m\ddot{x} + \left(\frac{12EI_x}{b^3}\right)x + \left(\frac{6EI_x}{b^2}\right)\xi = Q_x \qquad (18)$$

Σ forces parallel to the z axis at center of the disk:

$$+m\ddot{z} + \left(\frac{12EI_z}{b^3}\right) z - \left(\frac{12aEI_z}{b^3}\right) \theta - \left(\frac{6EI_z}{b^2}\right) \phi = Q_z \qquad (19)$$

Σ moments about the y axis at center of the disk:

$$+I_1\ddot{\theta} - I_2\Omega_1\dot{\phi} + I_2\Omega_2\dot{\xi} - \left(\frac{12aEI_z}{b^3}\right) z - \Omega_1^2 (I_2 - I_1)\theta + ma\Omega_1^2 z + \left(\frac{GJ}{b} + \frac{12a^2EI_z}{b^3}\right)\theta + \left(\frac{6aEI_z}{b^2}\right)\phi + I_2\Omega_1\Omega_2 = Q_\theta \qquad (20)$$

Σ moments about x axis at center of the disk:

$$+I_2\ddot{\phi} + I_1\Omega_1\dot{\theta} + mb\Omega_1^2 z - \left(\frac{6EI_z}{b^2}\right)z + \left(\frac{6aEI_z}{b^2}\right)\theta + \left(\frac{4EI_z}{b}\right)\phi - I_2\Omega_1\Omega_2\xi = Q_\phi \qquad (21)$$

Σ moments about z axis at center of disk:

$$+I_1\ddot{\xi} - I_2\Omega_2\dot{\theta} - mb\Omega_1^2 x + \left(\frac{6EI_x}{b^2}\right)x + \left(\frac{4EI_x}{b}\right)\xi = Q_\xi \qquad (22)$$

Equations (18) through (22) can be written in the matrix form of Equation (23) wherein the bending stiffness matrix for the cantilever bent is written separately from the stiffness matrices involving centrifugal force and gyroscopic moments.

The total polar mass moment of inertia, I_2, at each blade tip is 3.34 pound-inch-second^2, and the maximum angular velocity, Ω_2, of these rotating engine parts is 2,304 radians per second; and so the gyroscopic coupling terms in the damping matrix of Equation (23) will never exceed 10^4 inch-pounds per radian per second. The structural stiffness terms in the uncoupled moment equations (i.e., the diagonal stiffness terms) all exceed 10^7 inch-pounds per radian.

The relative significance of the gyroscopic coupling terms can be shown by rewriting the three moment equations using the operator 's' to denote a derivative with respect to time, d/dt, and expanding the resulting determinant in θ, ϕ and ξ to obtain the characteristic equation. It is immediately evident that the terms which contain Ω_2, the gyroscope rotational speed, are small in comparison with the structural stiffness terms and would not alter the roots of the characteristic equation. It is thus concluded that the gyroscopic effects of tip-mounted engines will not significantly alter either the natural frequencies or the mode shapes of a rotor blade which has the relative mass and stiffness properties of the one considered in the subject design.

$$
\begin{bmatrix} m & 0 & 0 & 0 & 0 \\ 0 & m & 0 & 0 & 0 \\ 0 & 0 & I_1 & 0 & 0 \\ 0 & 0 & 0 & I_2 & 0 \\ 0 & 0 & 0 & 0 & I_1 \end{bmatrix} \begin{Bmatrix} \ddot{x} \\ \ddot{z} \\ \ddot{\theta} \\ \ddot{\phi} \\ \ddot{\xi} \end{Bmatrix} + \begin{bmatrix} 0 & 0 & 0 & 0 & 0 \\ 0 & 0 & 0 & 0 & 0 \\ 0 & 0 & 0 & (-I_2\Omega_1) & (I_2\Omega_2) \\ 0 & 0 & (I_1\Omega_1) & 0 & 0 \\ 0 & 0 & (-I_2\Omega_2) & 0 & 0 \end{bmatrix} \begin{Bmatrix} \dot{x} \\ \dot{z} \\ \dot{\theta} \\ \dot{\phi} \\ \dot{\xi} \end{Bmatrix} +
$$

$$
\begin{bmatrix} 0 & 0 & 0 & 0 & 0 \\ 0 & 0 & 0 & 0 & 0 \\ 0 & 0 & \Omega_1^2(I_1-I_2) & 0 & 0 \\ 0 & 0 & 0 & 0 & (-I_2\Omega_1\Omega_2) \\ 0 & 0 & 0 & 0 & 0 \end{bmatrix} \begin{Bmatrix} x \\ z \\ \theta \\ \phi \\ \xi \end{Bmatrix} + \begin{bmatrix} 0 & 0 & 0 & 0 & 0 \\ 0 & 0 & 0 & 0 & 0 \\ 0 & (ma\Omega_1^2) & 0 & 0 & 0 \\ 0 & (mb\Omega_1^2) & 0 & 0 & 0 \\ (-mb\Omega_1^2) & 0 & 0 & 0 & 0 \end{bmatrix} \begin{Bmatrix} x \\ z \\ \theta \\ \phi \\ \xi \end{Bmatrix} +
$$

$$
\begin{bmatrix} \left(\frac{12EI_x}{b^3}\right) & 0 & 0 & 0 & \left(\frac{6EI_x}{b^2}\right) \\ 0 & \left(\frac{12EI_z}{b^3}\right) & \left(\frac{-12aEI_z}{b^3}\right) & \left(\frac{-6EI_z}{b^2}\right) & 0 \\ 0 & \left(\frac{-12aEI_z}{b^3}\right) & \left(\frac{GJ}{b} + \frac{12a^2EI_z}{b^3}\right) & \left(\frac{6aEI_z}{b^2}\right) & 0 \\ 0 & \left(\frac{-6EI_z}{b^2}\right) & \left(\frac{6aEI_z}{b^2}\right) & \left(\frac{4EI_z}{b}\right) & 0 \\ \left(\frac{6EI_x}{b^2}\right) & 0 & 0 & 0 & \left(\frac{4EI_x}{b}\right) \end{bmatrix} \begin{Bmatrix} x \\ z \\ \theta \\ \phi \\ \xi \end{Bmatrix} + \begin{Bmatrix} 0 \\ 0 \\ I_2\Omega_1\Omega_2 \\ 0 \\ 0 \end{Bmatrix} = \begin{Bmatrix} Q_x \\ Q_z \\ Q_\theta \\ Q_\phi \\ Q_\xi \end{Bmatrix} \qquad (23)
$$

4.5. Torsional Divergence

Torsional divergence of a lifting aerodynamic surface occurs when the rate of change of torque from external sources exceeds the rate of change of internal torque due to structural stiffness. A simplified approach to torsional divergence, used in this report, assumes no flapwise or in-plane motion of the rotor blade, whereas a more detailed approach to the problem would be to couple the flapwise, in-plane, and torsional motions of the blade.

The strain energy in torsion of a rotor blade which is restrained at the root by a finite control spring can be written as follows:

$$U = \frac{1}{2}\int_0^R GJ\left(\frac{d\theta}{dr}\right)^2 dr + \frac{1}{2} k_c \theta_o^2$$

or

$$U = \frac{1}{2}\int_0^R GJ\left(\frac{d\theta}{dr}\right)^2 dr + \frac{1}{2}\frac{T_o^2}{k_c} \qquad (24)$$

where: GJ = blade torsional stiffness, a function of radial position, $lb\text{-}in^2$

k_c = root control spring stiffness, in-lb/rad.

θ_o = pitch at the blade root

T_o = torsion at the blade root, θ_o/k_c

The potential energy associated with the aerodynamic lift and centrifugal centering moments can be written as follows:

$$P = \frac{1}{2}\int_0^R \Delta l\, e\theta\, dr + \frac{1}{2}\Delta l_T e_T \theta_T - \frac{1}{2}\int_0^R \Delta I_p \Omega^2 \theta^2 dr - \frac{1}{2}\Delta I_T \Omega^2 \theta_T^2 \qquad (25)$$

where: Δl = change in aerodynamic lift

e = distance of aerodynamic center forward of the blade elastic axis, in.

Ω = rotor angular velocity

ΔI_p = unit mass moment of inertia of a blade section about a vertical axis through the section feathering axis, $lb\text{-}in\text{-}sec^2/in.$

ΔI_T = Tip mass yawing mass moment of inertia less the rolling mass moment of inertia, $lb\text{-}in\text{-}sec^2$

Subscript T refers to tip mass.

The change in aerodynamic lift on a section of rotor blade can be written:

$$\Delta \ell = \frac{1}{2} \rho (r\Omega + v \sin \psi)^2 a \theta c \, dr$$

and for the tip mass

$$\Delta \ell_T = \frac{1}{2} \rho (R\Omega + v \sin \psi)^2 a_T A_T \theta_T$$

where: ρ = air density, slugs/ft^3
v = helicopter forward flight speed, f.p.s.
ψ = azimuth angle
a = lift curve slope, per radian
c = blade chord, assumed constant
A_T = reference lifting area of tip mass
θ = change of pitching angle

The average of the velocity squared at a radial distance r from the centerline of rotation can be written:

$$V^2 = \frac{1}{2\pi} \int_0^{2\pi} (r^2\Omega^2 + 2r\Omega v \sin \psi + v^2 \sin^2 \psi) \, d\psi$$

$$V^2 = r^2\Omega^2 + \frac{v^2}{2} = V_T^2 \left[\left(\frac{r}{R} \right)^2 + \frac{\mu^2}{2} \right]$$

Therefore:

$$\left.\begin{aligned} \Delta \ell &= \frac{1}{2} \rho a c V_T^2 \left(x^2 + \frac{\mu^2}{2}\right) \theta \, dr \\ \Delta \ell_T &= \frac{1}{2} \rho a_T A_T V_T^2 \left(1 + \frac{\mu^2}{2}\right) \theta_T \end{aligned}\right\} \qquad (26)$$

where: $x = r/R$
V_T = rotor tip speed, f.p.s.

A torsional deflection curve for the blade, as well as radial distributions of torsional stiffness and blade inertia properties, must be assumed. Assume that:

$$\theta = \theta_o + \theta_T \sin \frac{\pi x}{2}$$

$$GJ = GJ_o - \left(\frac{GJ_o - GJ_R}{R} \right) r = GJ_o (1 - \lambda_J x)$$

$$\Delta I_p = \Delta I_{p_o} - \left(\frac{\Delta I_{p_o} - \Delta I_{p_R}}{R} \right) r = \Delta I_{p_o} (1 - \lambda_I x)$$

where: $\lambda_J = 1 - GJ_R/GJ_o$
$\lambda_I = 1 - \Delta I_{p_R}/\Delta I_{p_o}$

Therefore: $$\frac{d\theta}{dr} = \frac{\pi}{2R}\,\theta_T \cos\frac{\pi x}{2}$$

Substituting the preceding expressions into Equations (24) and (25), integrating, and equating the strain energy to the potential energy gives the following expression for the speed at which torsional divergence occurs.

$$V_{T_D}^2 = \frac{\dfrac{\pi^2 GJ_o}{8R}\left[1-\dfrac{\lambda_J}{2}\left(1-\dfrac{4}{\pi^2}\right)\right]+k_c R_\theta^2+\Delta I_{p_o}\Omega^2\left\{\left(1-\dfrac{\lambda_I}{2}\right)R_\theta^2+\dfrac{2}{\pi}\left(1-\dfrac{2\lambda_I}{\pi}\right)R_\theta-\dfrac{1}{2}\left[1-\lambda_I\left(\dfrac{1}{2}+\dfrac{2}{\pi^2}\right)\right]-\dfrac{\Delta I_T}{\Delta I_{p_o}}\right\}}{\dfrac{1}{2}\rho acRe\left\{\left(\dfrac{1}{3}+\dfrac{\mu^2}{2}\right)R_\theta^2+\dfrac{1}{4}\left(\dfrac{8}{\pi}-\dfrac{16}{\pi^2}+\mu^2\right)R_\theta+\left(\dfrac{1}{6}+\dfrac{1}{\pi^2}+\dfrac{\mu^2}{4}\right)+\dfrac{a_T}{a}\left(\dfrac{A_T}{cR}\right)\dfrac{e_T}{e}\left(1+\mu^2\right)\right\}} \tag{27}$$

where: R_θ is the ratio of pitch angle change at the blade root to the pitch angle change at the blade tip.

Several observations can be made which allow Equation (27) to be greatly simplified.

a) The advance ratio $\mu = V/V_{T_D}$ at divergence is a very small number and the terms containing μ^2 are relatively unaffected if μ is assumed to be zero.

b) The centrifugal centering terms are stabilizing and the omission of the $\Delta I_{p_o}\Omega^2$ term is conservative for torsional divergence calculations.

c) The ratio $a_T A_T/acR$ is very small compared with other denominator terms and can be omitted.

Equation (27) can then be reduced to the following approximation:

$$V_{T_D}^2 = \frac{\pi^2 GJ_o\left[1-\dfrac{\lambda_J}{\pi^2}\left(1-\dfrac{4}{\pi^2}\right)\right]+8Rk_c R_\theta^2}{4\rho acR^2 e\left[\dfrac{R_\theta^2}{3}+\left(8-\dfrac{16}{\pi}\right)\dfrac{R_\theta}{\pi^2}+\left(\dfrac{1}{6}+\dfrac{1}{\pi^2}\right)\right]} \tag{28}$$

For any finite value of k_c the ratio R_θ must be less than unity; and for an infinitely stiff root spring, $R_\theta = 0$ since the pitch at the blade root cannot change. Section 4.3.2 indicates that for $k_c = 10^8$ inch-pounds per radian, which is the design value, the major portion of the torsional deflection is due to blade twist, and so R_θ can be assumed to be less than 0.1.

Using:

$GJ_o = 12(10^9)$ lb-in^2

$\lambda_J = 0.75$ (Reference Figure 5)

$k_c = 10^8$ in-lb/rad.

$R_\theta = 0.1$

$\rho = .002378$ slugs/ft^3 (sea level)

$a = 5.73$ per rad.

$c = 6.5$ ft.

$R = 56$ ft. $= 672$ in.

Equation (28) can be reduced to:

$$V_{T_D}^2 = \frac{92(10)^9 + 5.4(10)^9}{13{,}332(0.3008)e} = \frac{24.3(10)^6}{e} \ , \ \frac{ft^2}{sec^2}$$

$$V_{T_D} = \frac{4930}{\sqrt{e}} \text{ f.p.s.}$$

where e is dimensioned in inches.

The rotor blade which is proposed for the heavy-lift tip turbojet helicopter is designed with most of the torsion-carrying material forward of the semichord, and the shear center is estimated to be slightly forward of the blade quarter chord. Since pure torsional divergence cannot occur if e is negative, it is doubtful that there is a finite torsional divergence tip speed since the aerodynamic center for an NACA 0015 airfoil section is nominally taken at either the 24- or 25-percent-chord point. If the shear center were located as far aft as 50 percent of the chord, the torsional divergence tip speed would still be safely above the design tip speed.

The static stability of the subject rotor design, including the effects of in-plane and out-of-plane bending, is further assured as a result of the analog computer simulation described in Reference 1. This simulation included in-plane and out-of-plane conditions (i.e., 2.5g pullup) which result in the highest in-plane and out-of-plane deflections. If static instability were present in the rotor, it would have become evident during these studies.

4.6 Special Dynamic Considerations

There are two dynamic considerations worthy of discussion which are peculiar to the large tip turbojet helicopter. One of these concerns the very low design rotor speed and the possibility of inadvertent cycling of the controls so as to excite the first cyclic in-plane mode of the rotor

blades. The second consideration involves sling suspension of the cargo and its possible dynamic consequences.

4.6.1 Cyclic Stick Whirl

Reference 1 points out the fact that it is well within pilot capability to cycle the controls at such a frequency as to excite the first cyclic in-plane mode of the rotor blades and cause high in-plane bending moments. For the case considered in Reference 1, the first cyclic in-plane frequency is 1.247 cycles per revolution in the rotating system and, hence, 0.247 cycles per revolution in the nonrotating system at the cyclic control stick. This relationship of rotating frequency less one cycle per revolution equalling the frequency in the nonrotating system is immediately obvious when one considers that a steady cyclic pitch input by the pilot causes a one-cycle-per-revolution input of cyclic pitch to the blades. For a nominal hovering rotor speed of 11.6 radians per second (= 1.846 cycles per second), it is seen that a rotary motion of the cyclic pitch control of 0.247(1.846) = 0.46 cycles per second will excite the first in-plane mode.

It is concluded that the avoidance of cyclic stick whirl by the pilot cannot logically be assumed even though the phenomenon is recognized as undesirable, and so the peak in-plane bending moments shown in Reference 1 must be considered for rotor blade design.

4.6.2 Sling Load

Reference 3 considers the useful load (cargo) to be secured to the helicopter fuselage so that the cargo mass is merely considered to be added fuselage mass for helicopter stability calculations. It is also envisioned that the cargo mass could be carried on a sling suspended below the helicopter as shown in Figure 4.

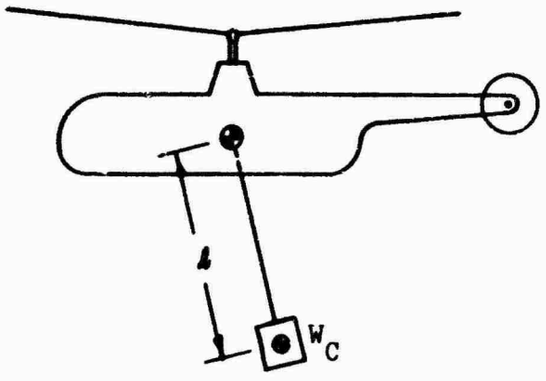

Figure 4. Cargo Sling Load.

The linearized equations of motion of Reference 3 for a hovering helicopter have been altered to include the sling load, and the frequency results of this study verify that the cargo and sling behave like a simple pendulum. The sling length was varied from 16 feet to 200 feet with a cargo weight of 24,000 pounds, and the frequency of the slung cargo was found to vary between 1.3 radians per second to 0.4 radians per second for the sling lengths noted. Thus, there is little chance that the sling length will ever be short enough to produce frequencies which approach the rotor blade natural frequencies; and therefore, it is concluded that a conventional sling load will not affect the dynamics of the rotor blades.

4.7 Rotor Blade Flutter

A study of rotor blade flutter and dynamic response characteristics has been conducted and is completely documented in Reference 1. This study was conducted for the purpose of determining rotor parameter variations on flutter as well as to evaluate the effect of tip-mounted turbojet engines on blade dynamics.

So that the effects of rotor-induced inflow, blade deflection, and collective pitch could be included in the variation of parameters, four flight conditions were assumed. These conditions are as follows:

a) 1g hover at W_G = 71,680 lb.
b) 2.5g vertical acceleration at W_G = 71,680 lb.
c) Maximum vertical rate of climb at W_G = 71,680 lb.
d) Minimum collective pitch ($\theta_{.75R}$ = -5 deg.)

Conditions b) and d) are not completely realistic flight conditions since the rotor cannot develop 2.5g of thrust in hover, nor will the collective pitch limit be less than zero degrees at 0.75R. These conditions are included, however, since they represent conservative boundary conditions for positive and negative inflow. Figures 12 and 13 present estimated curves of blade deflection and rotor inflow velocity, respectively, for the four conditions under consideration, and Table 4 defines collective pitch settings, turbojet engine thrust, and turbine speed (r.p.m.) for each condition. Figures 5 and 6 present the stiffness and mass data that are required for the flutter study. Some of the pertinent data which are held constant throughout the study are as follows:

Ω = rotor angular velocity, 11.62 rad/sec.
θ_T = blade twist, -10 deg.
R = rotor radius, 56 ft.
a_o = precone angle, 1.2 deg.
W_T = tip weight, 1,200 lb. per blade
Tip engine mass properties
Chordwise center of gravity, 0.25c

The parameters which were varied during the study, and the ranges of variation, are as follows:

k_c = root control spring stiffness, 5×10^7 to 15×10^7 in-lb/rad.

δ_3 = delta three angle, 0 to 45 deg.

ω_E = turbine (engine) speed, -66,000 to +66,000 r.p.m.

c = blade chord, 5.5 ft., 6.5 ft.

Shear center, 0.20c to 0.25c

Tip mass chordwise c.g., 0.16c to 0.28c

Flapwise EI of rotor blade
Chordwise EI of rotor blade
Weight distribution of rotor blade

} Compatible with blade chord, c

The rotor blade simulation and direct analog computer circuitry are explained in detail in Reference 1 and are not repeated here. The method used to evaluate the stability of each configuration tested is also documented in Reference 1, but will be repeated here to aid in the interpretation of those curves which are taken from Reference 1 and reproduced herein for convenience.

The aerodynamic damping for each rotor blade configuration and natural frequency is obtained by driving the analog computer circuit with an oscillating voltage source. The drive point is selected to give large response in the desired mode and small response in the other modes. The mode frequency is determined as the frequency at which the drive current is a minimum (corresponding to minimum force for a given drive velocity). The damping is determined from the shape of the current versus frequency curve near the resonant frequency. The damping factor, G, is numerically equal to twice the per-unit critical damping factor, ζ. Because inherent damping exists in every analog computer circuit, each rotor blade configuration was tested both with and without aerodynamics so that the damping due to the analog circuitry could be subtracted from the total damping to yield only that damping which is attributable to aerodynamics.

No attempt has been made in Reference 1 to add structural damping to the rotor blade simulation, and so a value is assumed for discussion purposes only. It is not uncommon to achieve structural damping factors of $\zeta = .015$ (per-unit critical damping) in dynamic systems which are constructed entirely of metallic components as is the tip turbojet rotor blade. Based on the assumption that $\zeta_s = .015$ for this rotor blade, then, the structural damping is assumed to be

$$G_s = 2\,\zeta_s = .03 \quad \text{(structural damping)}$$

Before discussing the effect of variation of parameters on blade flutter, it is well to note that the only mode of vibration which has negative

aerodynamic damping, using the nominal blade parameters, is the second cyclic mode for the 2.5g hover condition and the maximum negative collective pitch condition. Aside from the fact that the assumed structural damping is more than adequate to make this mode stable, it is pointed out that these two conditions are not realistic, as was mentioned previously. The 1g hover and maximum vertical climb conditions have no unstable modes, even excluding structural damping.

The influence of root control spring stiffness, k_c, on blade flutter is best shown for the second cyclic and second collective modes, the only modes for which aerodynamic damping becomes more negative (destabilizing) with increasing control spring flexibility. The 2.5g hover condition is shown since the aerodynamic damping is most destabilizing for this condition. Figure 14 points out the need for a control spring stiffness at least equal to the blade torsional stiffness to avoid flutter if the structural damping factor is assumed to be .03 as previously discussed. This requirement is easily met since the design goal at present is for a stiffness ratio of 10:1 (flexibility ratio of 1:10).

The effect of the tip weight, chordwise, center-of-gravity-position is also shown in Figure 14. It is apparent that an extreme travel of the tip weight center of gravity either fore or aft on the blade does not affect all modes in the same way. Whereas the second collective mode is more stable for an aft tip weight center of gravity, the second cyclic mode is more stable for a forward center of gravity location. Present design calls for a tip weight center-of-gravity placement at the 22-percent chord point and so a compromise is affected for both modes.

A variation of δ_3 angle (pitch-flap coupling) affects only the second cyclic mode adversely and results in the largest negative aerodynamic damping for the 2.5g hover condition. Figure 15 shows the effect of increasing δ_3 angle on aerodynamic damping for this mode. Assuming a structural damping factor of .03 guarantees avoidance of flutter for δ_3 angles up to 45 degrees. Present design shows no advantage to pitch-flap coupling angles approaching 45 degrees, and so the present design calls for a δ_3 angle of 10 degrees.

The effect of chordwise location of the blade elastic axis is also shown in Figure 15. The tendency toward a more stable dynamic system for a more forward elastic axis is indicated both from Figure 15 and elsewhere in Reference 1, at least for the second cyclic mode. The other modes are not of immediate interest since they all possess positive aerodynamic damping when using nominal blade parameters. The elastic axis for the existing blade design is estimated to be forward of the quarter chord and, hence, in the proper location to reduce the aerodynamic instability of the second cyclic mode.

The rotational speed and direction of turbine rotation of the tip-mounted engines is concluded to have a negligible effect on blade flutter in Ref-

erence 1. The general trend is for turbine rotation in either direction to increase the damping. For the modes where this generalization does not apply, the change in aerodynamic damping up to maximum turbine speed in either direction is less than $\Delta G = -.004$ when using nominal rotor blade properties.

The influence of blade chord (or blade aspect ratio) on flutter was not systematically investigated through a range of dimensions since subtle changes in blade stiffness and distributed weight must accompany changes in chord in order to be realistic. As an alternative procedure, however, the estimated rotor blade parameters for a 5.5-foot-chord blade and a 6.5-foot-chord blade were calculated and the aerodynamic damping factors compared for similar flight conditions. Table 3 presents a comparison of the aerodynamic damping factors, G, for the 1g hover and 2.5g hover conditions. These cases are chosen since they all have shear centers located at 0.25 chord and tip weight center-of-gravity locations at 0.22 chord. All other variables such as control spring stiffness, δ_3 angle, engine turbine speed, rotor speed, tip weight, and blade twist are the same for all cases. Those variables which are influenced by rotor solidity, such as collective pitch, have been calculated for each case.

TABLE 3
BLADE CHORD INFLUENCE ON AERODYNAMIC DAMPING

Mode	Aerodynamic Damping Factor, G			
	1g Hover		2.5g Hover	
	c = 5.5 ft.	c = 6.5 ft.	c = 5.5 ft.	c = 6.5 ft.
1st cyclic	.300	*	.307	*
2nd "	-.004	.030	0	-.014
3rd "	.079	.116	.075	.109
4th "	.017	.045	.018	.027
5th "	.016	*	.009	*
6th "	.141	.029	.140	.012
1st collective	.288	*	.324	*
2nd "	.079	.120	.070	.096
3rd "	-.002	.028	.020	.015
4th "	.005	.257	.015	.238
5th "	*	.073	*	.064
6th "	)22	.035	.013	.002

* Not available in Reference 1.

The 6.5-foot-chord blade has more aerodynamic damping for every mode except the sixth cyclic for the 1g hover condition and has more damping for every mode except the second cyclic, sixth cyclic, and sixth collective

for the unrealistic 2.5g hover condition. Reference 4 states that for moderate values of torsional structural damping (G = .03), a design flutter parameter ($c\omega_\alpha/2a$) in excess of 0.3 should guarantee flutter-free operation. In this expression, c = blade chord, ω_α = first nonrotating torsional natural frequency, a = speed of sound at sea level. This design flutter parameter varies directly with blade chord and supports the conclusion drawn from Table 3 that the larger chord blade provides more aerodynamic damping for a majority of modes.

The influence of a blade root flapwise stiffness (EI) buildup on aerodynamic damping for the 6.5-foot-chord blade has been shown in Reference 1. Once again, the 1g hover and 2.5g hover conditions can be compared for identical blade parameters to show that the aerodynamic damping increases slightly with increasing flapwise EI, but the change is so small as to be of academic interest only.

Reference 1 presents several different blade parameter variations than are discussed here, but none of these variations indicate a significant tendency toward instability. A summary conclusion for the work described in Reference 1 indicates that the rotor blades are flutter-free for the nominal four-bladed rotor design proposed in this report.

TABLE 4
ROTOR OPERATING DATA

Condition	Collective Pitch at 0.75R	Tip Engine Thrust*	Tip Engine Speed
1g hover	+8.5 deg.	2,020 lb.	20,250 r.p.m.
2.5g hover	+16.5 deg.	‡3,080 lb.	22,000 r.p.m.
Max. vertical rate of climb	+13.1 deg.	3,080 lb.	22,000 r.p.m.
Max. negative coll. pitch	-5.0 deg.	1,060 lb.	18,700 r.p.m.

* Total for two engines.

‡ Maximum available thrust, not sufficient to maintain Ω = 11.62 rad/sec. (Equilibrium thrust = 6,040 lb/tip.)

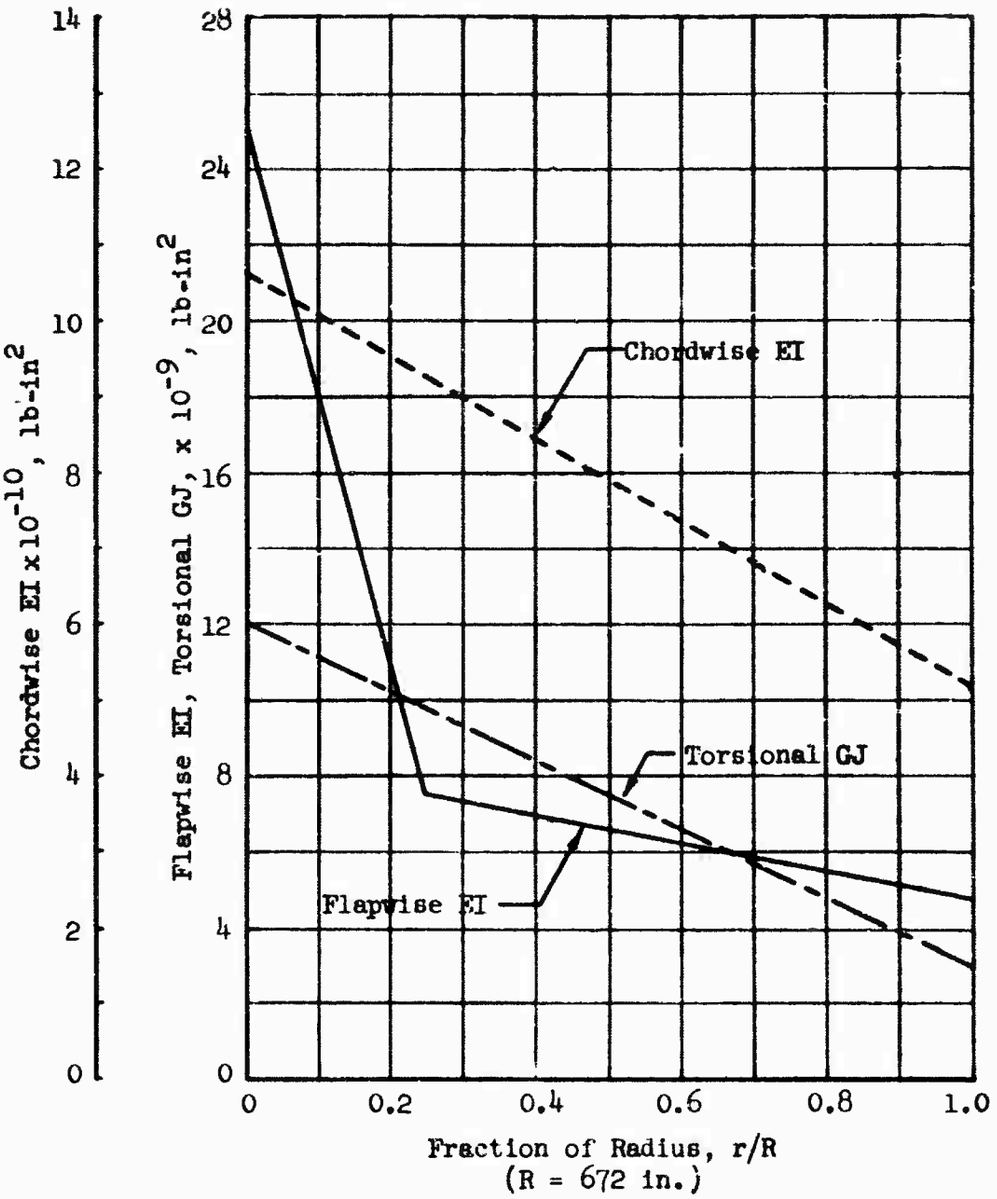

Figure 5. Rotor Blade Stiffness (EI, GJ) Versus Radius.

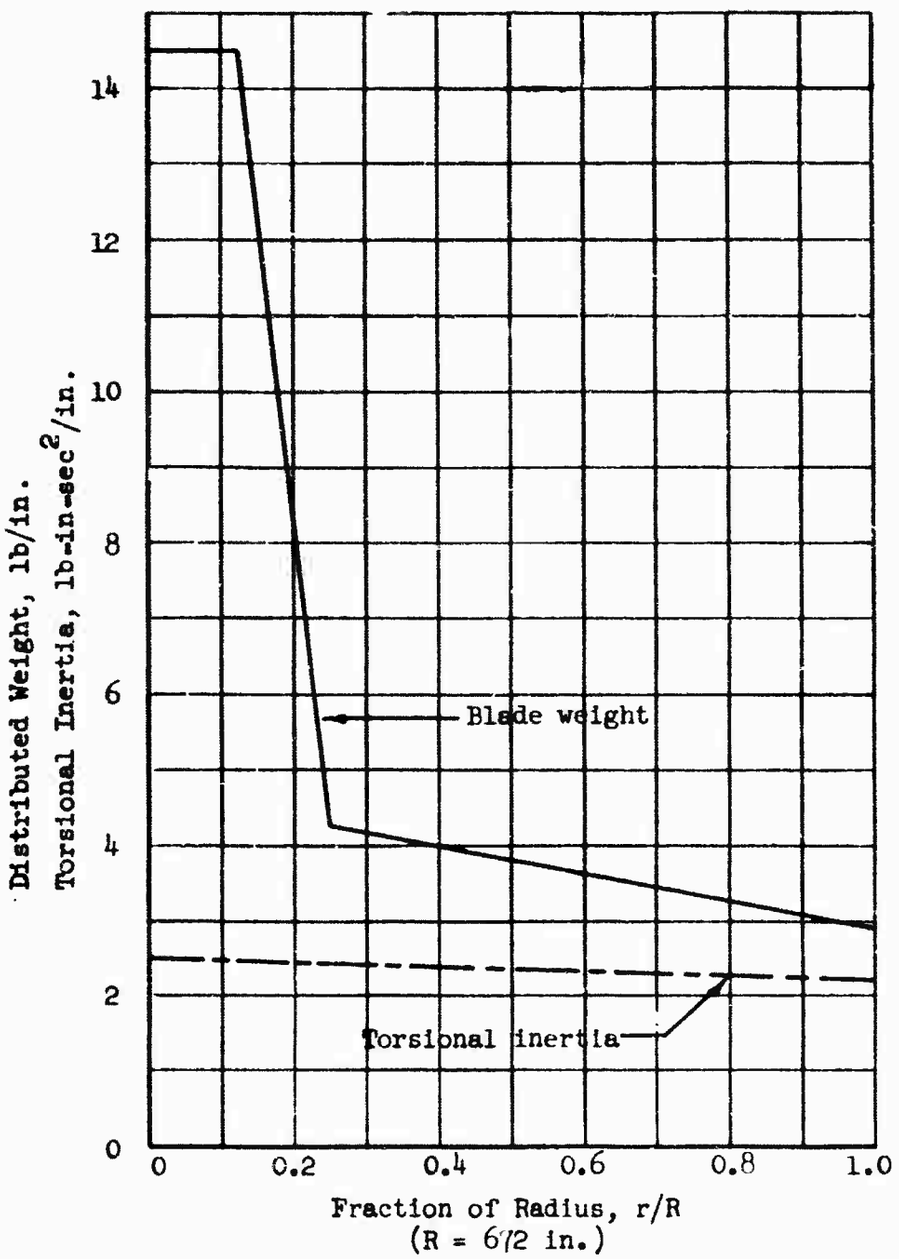

Figure 6. Rotor Blade Weight and Torsional Inertia Versus Radius.

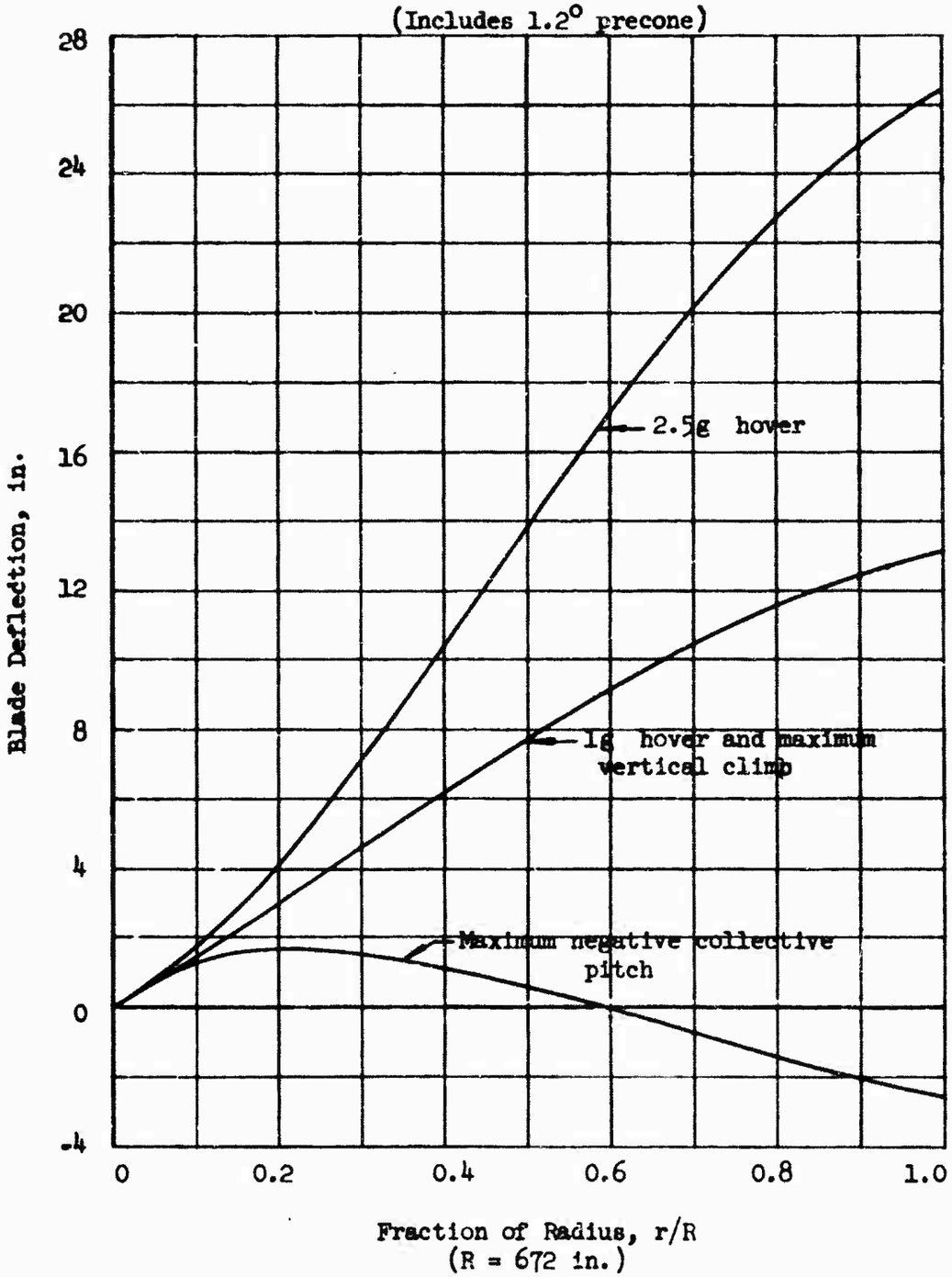

Figure 7. Blade Deflection Versus Radius.

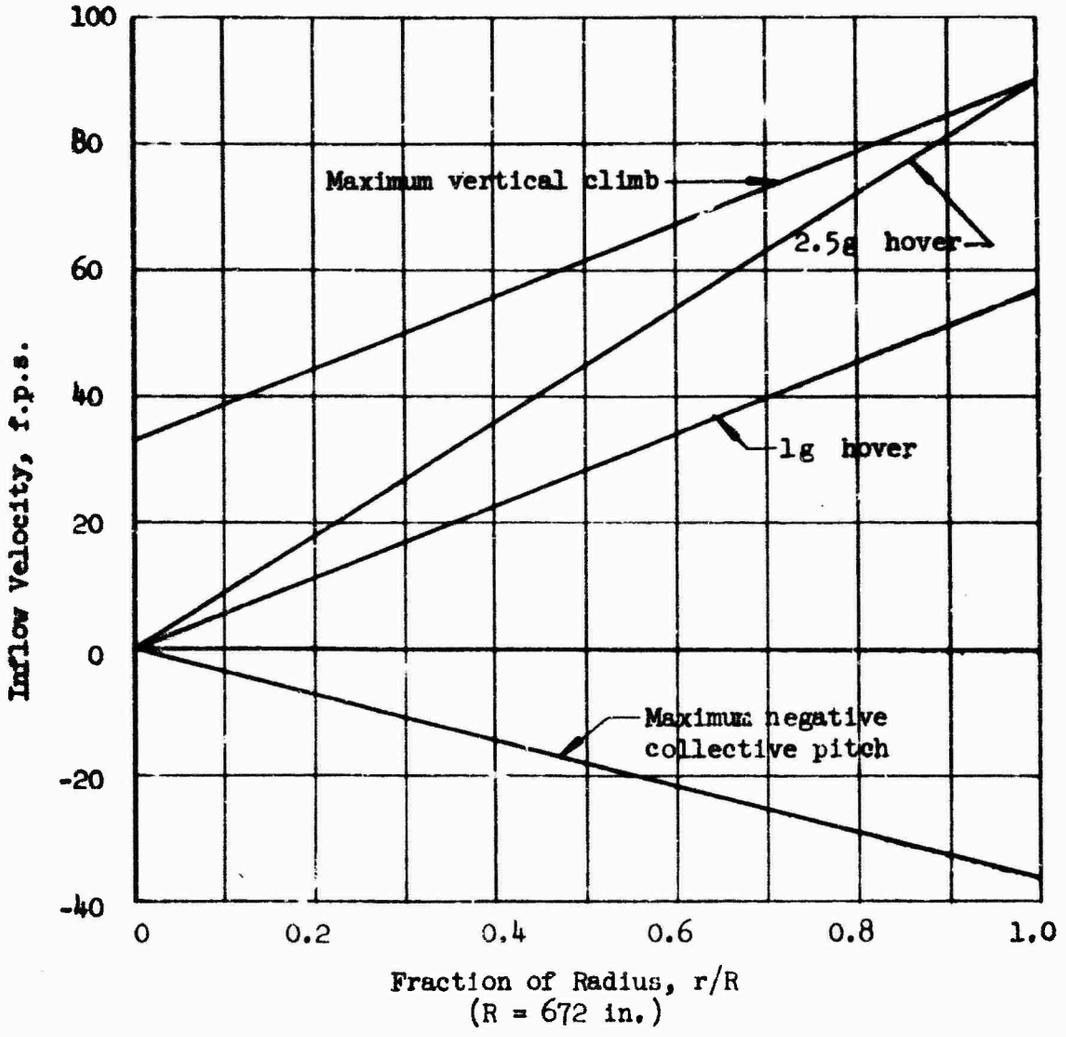

Figure 8. Inflow Velocity Versus Radius.

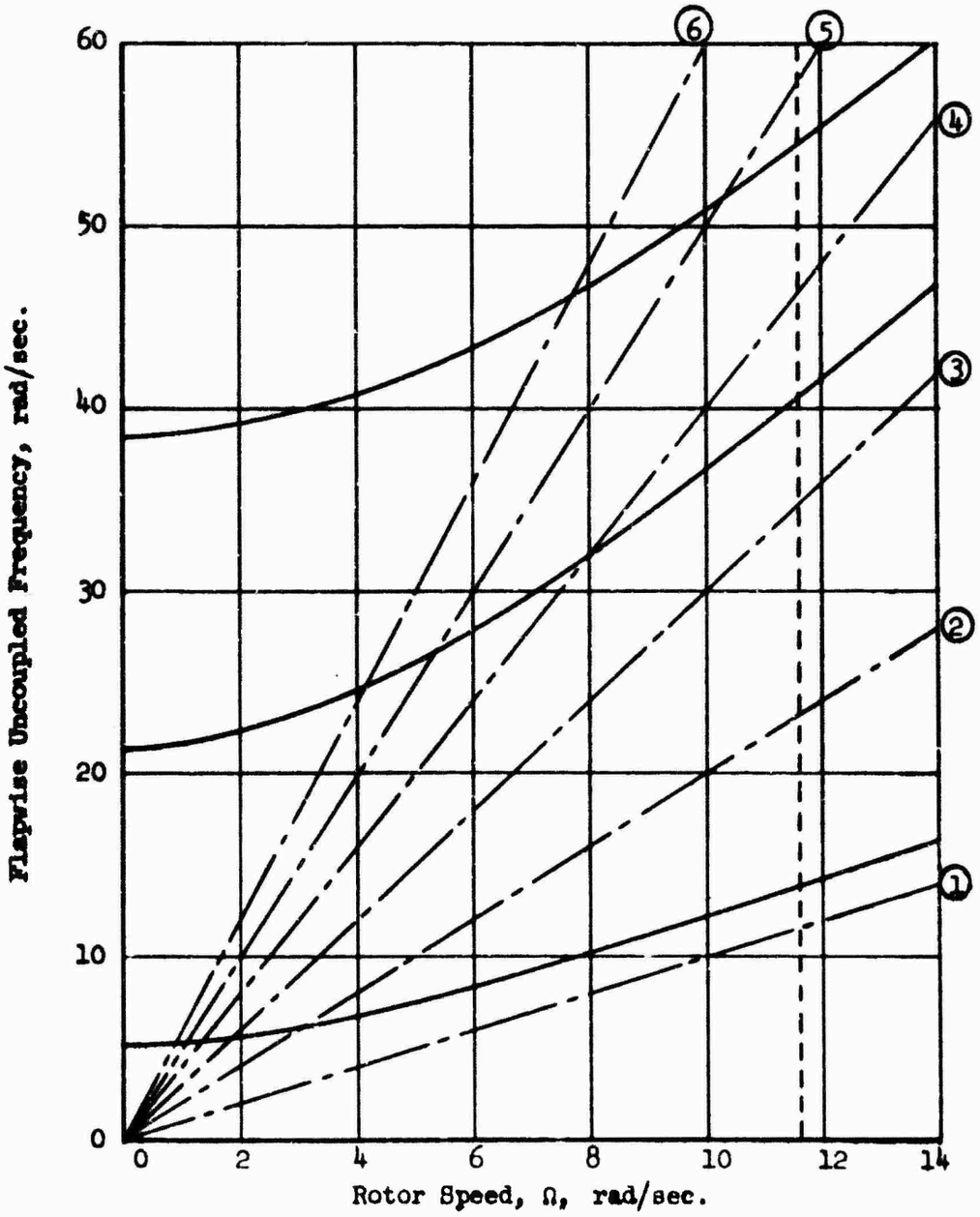

Figure 9. Flapwise Uncoupled Frequency Versus Rotor Speed .

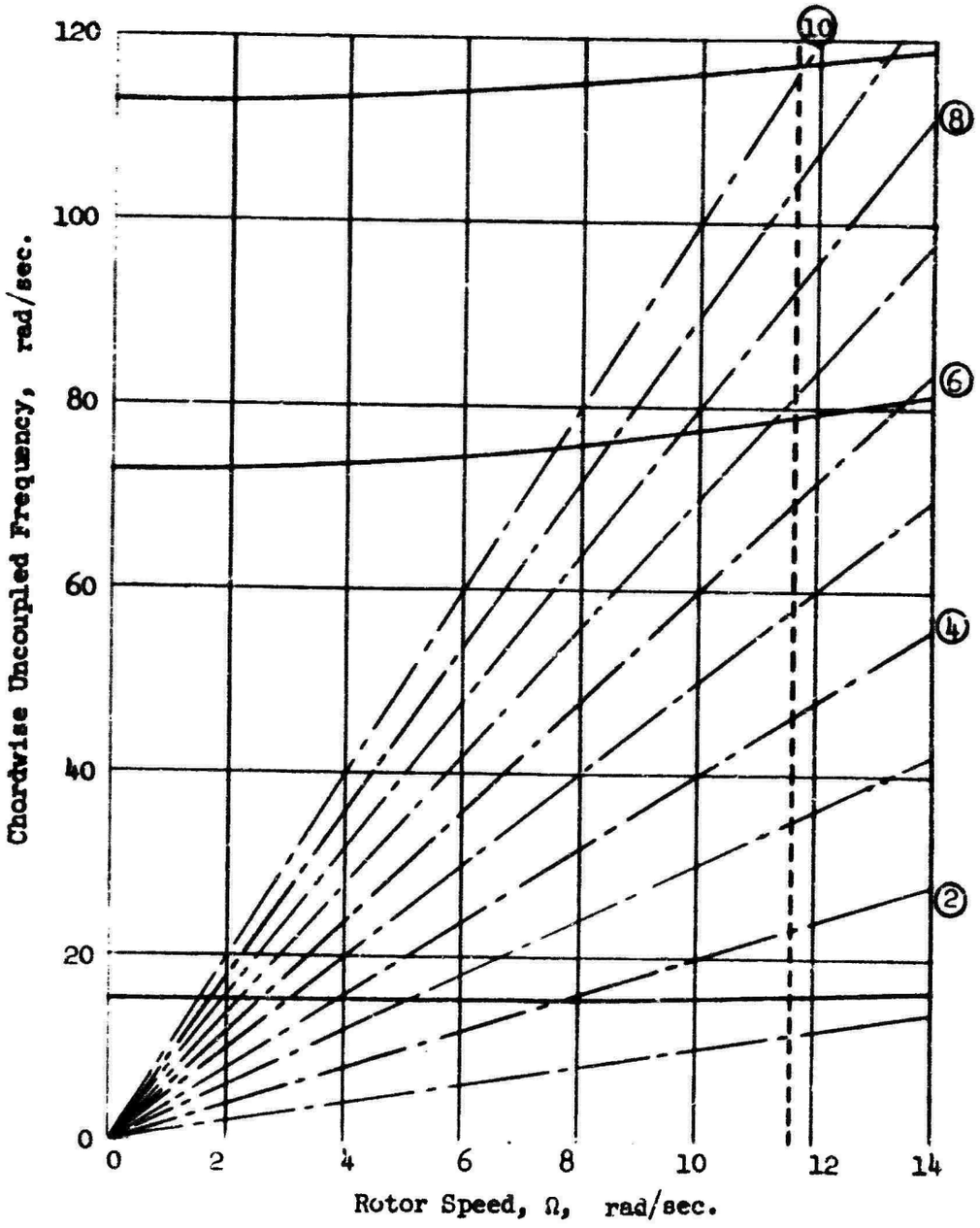

Figure 10. Chordwise Uncoupled Frequency Versus Rotor Speed.

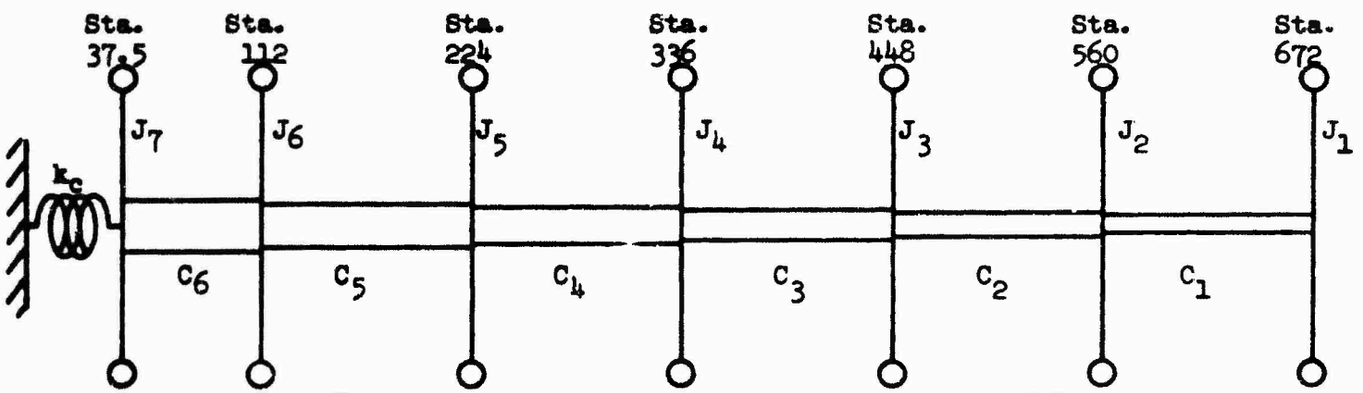

Inertia Values		Stiffness Values	
J_1 = 337,560	lb-in^2	C_1 = 33 x 10^6	in-lb/rad.
J_2 = 98,350	"	C_2 = 47 x 10^6	"
J_3 = 100,300	"	C_3 = 60 x 10^6	"
J_4 = 102,240	"	C_4 = 74 x 10^6	"
J_5 = 104,190	"	C_5 = 87 x 10^6	"
J_6 = 106,130	"	C_6 = 148 x 10^6	"
J_7 = 17,500	"	k_c = 100 x 10^6	"

Figure 11. Equivalent Torsional System.

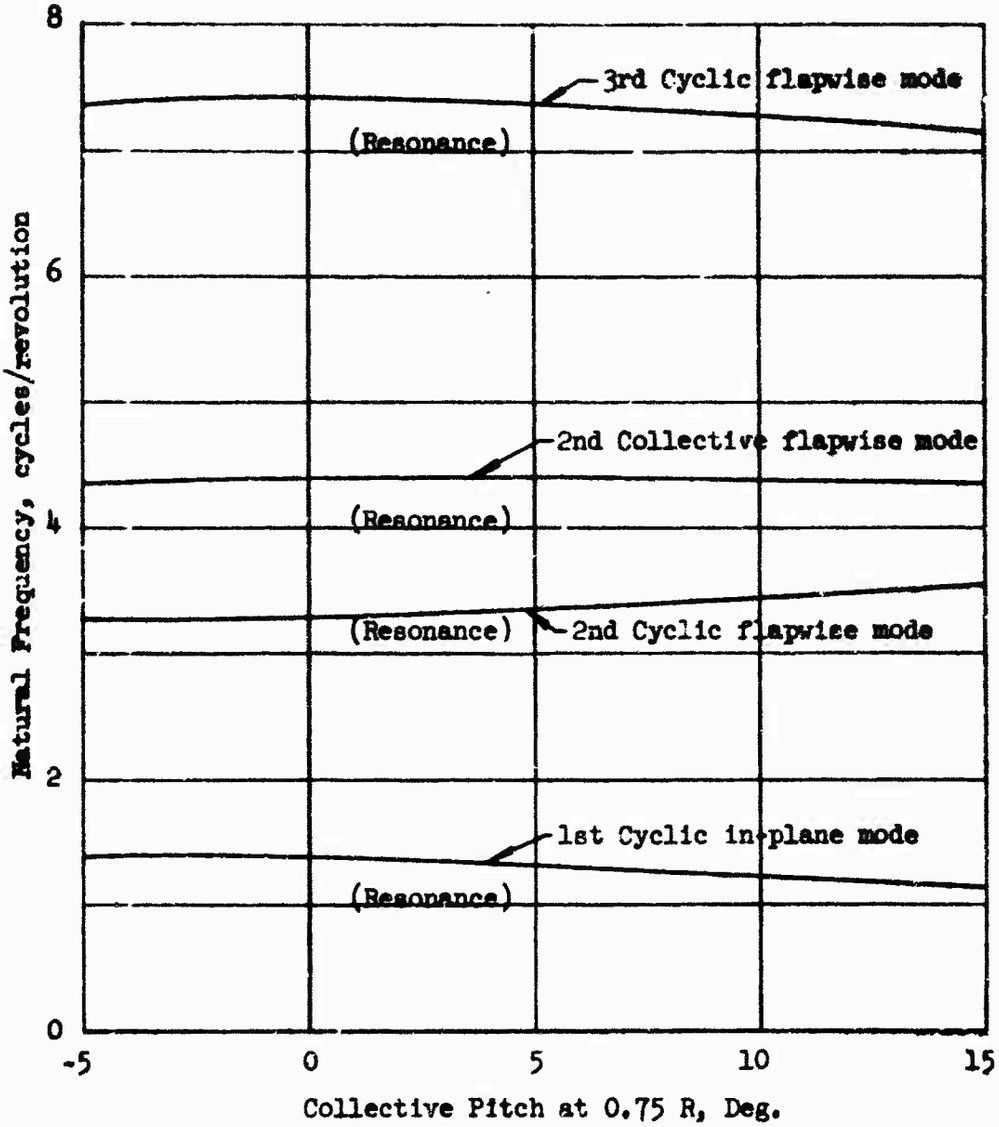

Figure 12. Coupled Natural Frequency Versus Collective Pitch.

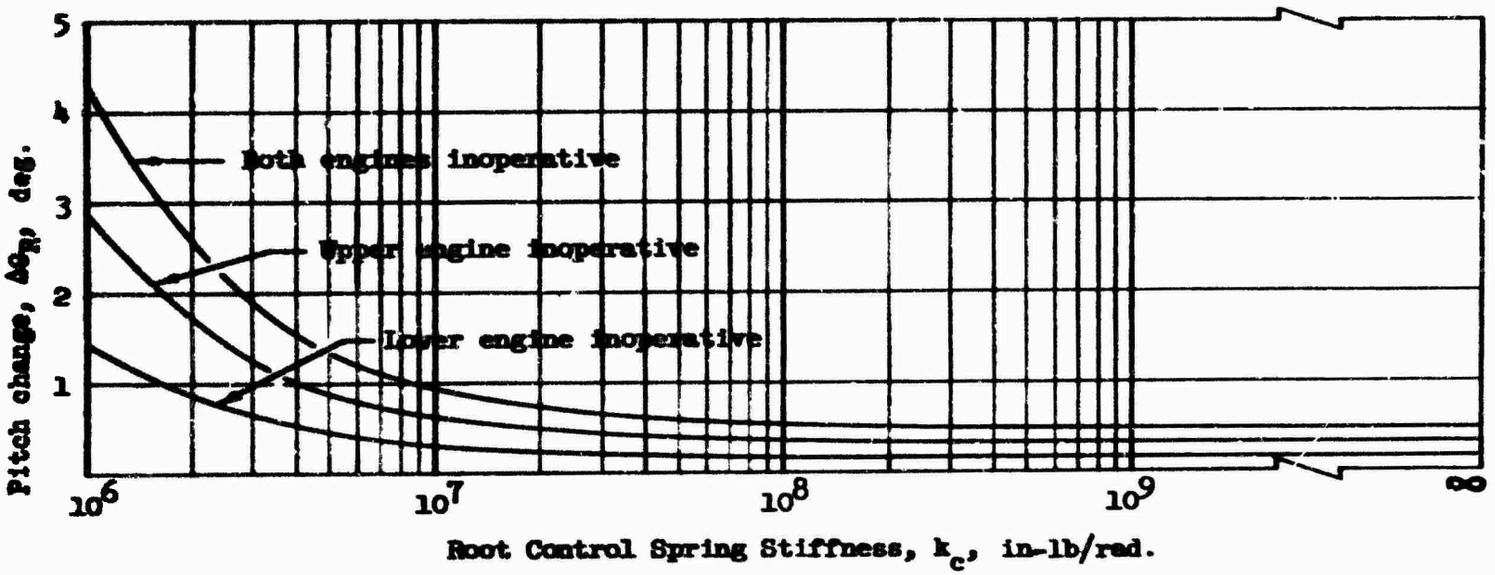

Figure 13. Blade Tip Pitch Change Versus Control Spring Stiffness - Engine Failure Condition.

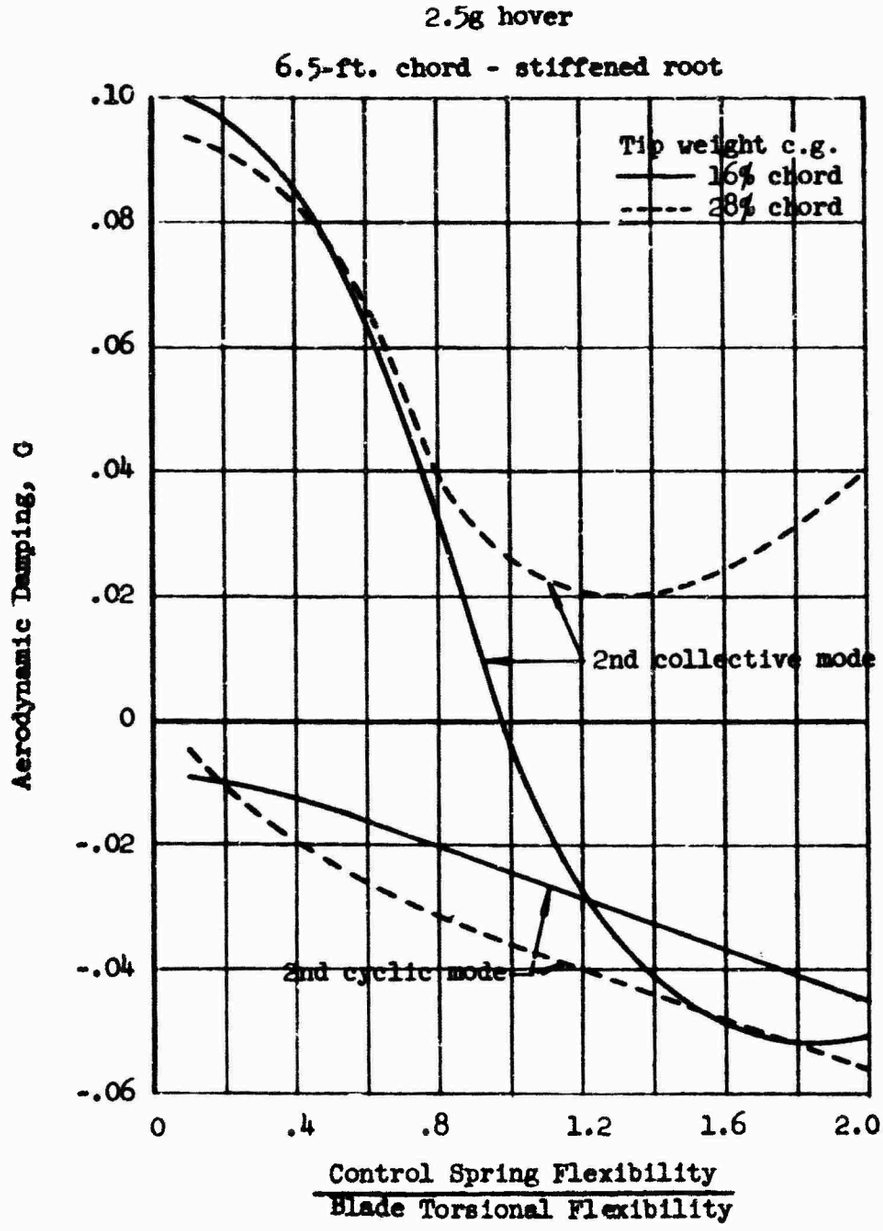

Figure 14. Aerodynamic Damping Versus Control Spring Flexibility.

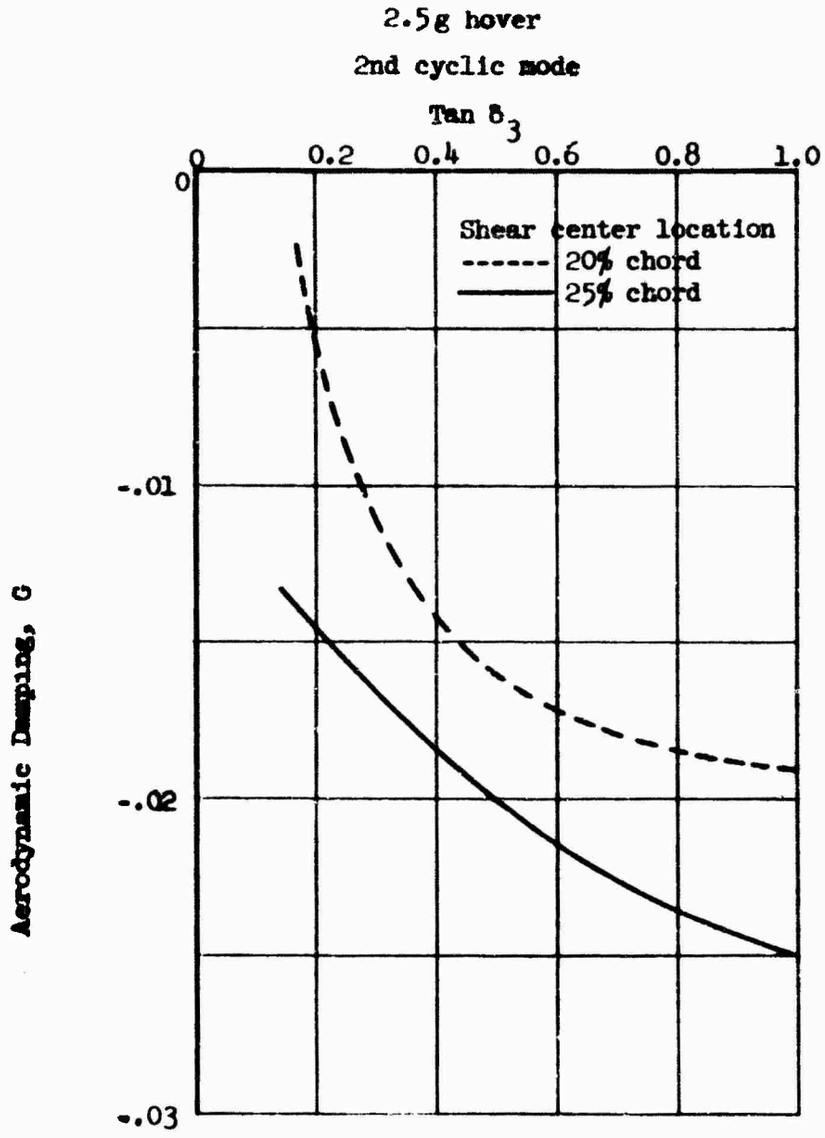

Figure 15. Aerodynamic Damping Versus Pitch-Flap Coupling (δ_3).

5.0 REFERENCES

1. Direct Analog Computer Study of a Tip Turbojet Rotor System, The MacNeal-Schwendler Corporation, San Marino, California, February 1964. (Available at U. S. Army Transportation Research Command,* Fort Eustis, Virginia.)

2. Scanlon, R. H., and Rosenbaum, R., Introduction to the Study of Aircraft Vibration and Flutter, The MacMillan Co., New York, N. Y., 1951.

3. "Stability and Control," Heavy-Lift Tip Turbojet Rotor System, Volume X, Hiller Engineering Report No. 64-50, U. S. Army Transportation Research Command,* Fort Eustis, Virginia, October 1965.

4. Brooks, G. W., and Baker, J. E., "An Experimental Investigation of the Effect of Various Parameters Including Tip Mach Number on the Flutter of Some Model Helicopter Rotor Blades," NACA TN 4005,

*Changed to U. S. Army Aviation Materiel Laboratories, March 1965.

Unclassified

Security Classification

DOCUMENT CONTROL DATA - R&D

(Security classification of title, body of abstract and indexing annotation must be entered when the overall report is classified)

1. ORIGINATING ACTIVITY (Corporate author)

Hiller Aircraft Company, Inc.
Palo Alto, California

2a. REPORT SECURITY CLASSIFICATION

Unclassified

2b. GROUP

3. REPORT TITLE

Heavy-Lift Tip Turbojet Rotor System, "Dynamic and Aeroelastic Studies", Volume VI

4. DESCRIPTIVE NOTES (Type of report and inclusive dates)

5. AUTHOR(S) (Last name, first name, initial)

6. REPORT DATE	7a. TOTAL NO. OF PAGES	7b. NO. OF REFS
October 1965	47	4

8a. CONTRACT OR GRANT NO.	9a. ORIGINATOR'S REPORT NUMBER(S)
DA 44-177-AMC-25(T) b. PROJECT NO. Task 1M121401D14412 c. d.	USAAVLABS Technical Report 64-68F 9b. OTHER REPORT NO(S) (Any other numbers that may be assigned this report) Hiller Engineering Report 64-46

10. AVAILABILITY/LIMITATION NOTICES

Qualified requesters may obtain copies of this report from DDC.
This report has been furnished to the Department of Commerce for sale to the public.

11. SUPPLEMENTARY NOTES	12. SPONSORING MILITARY ACTIVITY
	US Army Aviation Materiel Laboratories Fort Eustis, Virginia

13. ABSTRACT

In Volume VI of Heavy-Lift Tip Turbojet Rotor System, the dynamic and aeroelastic properties of the rotor blades are presented with particular emphasis on the effect of tip-mounted turbojet engines on flutter. A variation of parameter study, conducted on a direct analog computer, is also discussed.

DD FORM 1 JAN 64 1473

Unclassified

Security Classification

Unclassified

Security Classification

14. KEY WORDS	LINK A		LINK B		LINK C	
	ROLE	WT	ROLE	WT	ROLE	WT
Tip Turbojet Rotor System Dynamic and Aeroelastic Studies						

INSTRUCTIONS

1. ORIGINATING ACTIVITY: Enter the name and address of the contractor, subcontractor, grantee, Department of Defense activity or other organization *(corporate author)* issuing the report.

2a. REPORT SECURITY CLASSIFICATION: Enter the overall security classification of the report. Indicate whether "Restricted Data" is included. Marking is to be in accordance with appropriate security regulations.

2b. GROUP: Automatic downgrading is specified in DoD Directive 5200.10 and Armed Forces Industrial Manual. Enter the group number. Also, when applicable, show that optional markings have been used for Group 3 and Group 4 as authorized.

3. REPORT TITLE: Enter the complete report title in all capital letters. Titles in all cases should be unclassified. If a meaningful title cannot be selected without classification, show title classification in all capitals in parenthesis immediately following the title.

4. DESCRIPTIVE NOTES: If appropriate, enter the type of report, e.g., interim, progress, summary, annual, or final. Give the inclusive dates when a specific reporting period is covered.

5. AUTHOR(S): Enter the name(s) of author(s) as shown on or in the report. Enter last name, first name, middle initial. If military, show rank and branch of service. The name of the principal author is an absolute minimum requirement.

6. REPORT DATE: Enter the date of the report as day, month, year, or month, year. If more than one date appears on the report, use date of publication.

7a. TOTAL NUMBER OF PAGES: The total page count should follow normal pagination procedures, i.e., enter the number of pages containing information.

7b. NUMBER OF REFERENCES: Enter the total number of references cited in the report.

8a. CONTRACT OR GRANT NUMBER: If appropriate, enter the applicable number of the contract or grant under which the report was written.

8b, 8c, & 8d. PROJECT NUMBER: Enter the appropriate military department identification, such as project number, subproject number, system numbers, task number, etc.

9a. ORIGINATOR'S REPORT NUMBER(S): Enter the official report number by which the document will be identified and controlled by the originating activity. This number must be unique to this report.

9b. OTHER REPORT NUMBER(S): If the report has been assigned any other report numbers *(either by the originator or by the sponsor)*, also enter this number(s).

10. AVAILABILITY/LIMITATION NOTICES: Enter any limitations on further dissemination of the report, other than those imposed by security classification, using standard statements such as:

(1) "Qualified requesters may obtain copies of this report from DDC."

(2) "Foreign announcement and dissemination of this report by DDC is not authorized."

(3) "U. S. Government agencies may obtain copies of this report directly from DDC. Other qualified DDC users shall request through _____."

(4) "U. S. military agencies may obtain copies of this report directly from DDC. Other qualified users shall request through _____."

(5) "All distribution of this report is controlled. Qualified DDC users shall request through _____."

If the report has been furnished to the Office of Technical Services, Department of Commerce, for sale to the public, indicate this fact and enter the price, if known.

11. SUPPLEMENTARY NOTES: Use for additional explanatory notes.

12. SPONSORING MILITARY ACTIVITY: Enter the name of the departmental project office or laboratory sponsoring *(paying for)* the research and development. Include address.

13. ABSTRACT: Enter an abstract giving a brief and factual summary of the document indicative of the report, even though it may also appear elsewhere in the body of the technical report. If additional space is required, a continuation sheet shall be attached.

It is highly desirable that the abstract of classified reports be unclassified. Each paragraph of the abstract shall end with an indication of the military security classification of the information in the paragraph, represented as *(TS)*, *(S)*, *(C)*, or *(U)*.

There is no limitation on the length of the abstract. However, the suggested length is from 150 to 225 words.

14. KEY WORDS: Key words are technically meaningful terms or short phrases that characterize a report and may be used as index entries for cataloging the report. Key words must be selected so that no security classification is required. Identifiers, such as equipment model designation, trade name, military project code name, geographic location, may be used as key words but will be followed by an indication of technical context. The assignment of links, rules, and weights is optional.

Unclassified

Security Classification

6493-65